The Aggregatibacter actinomycetemcomitans cytolethal distending toxin active subunit, CdtB, contains a cholesterol recognition sequence required for toxin binding and subunit internalization

Authors: Kathleen Boesze-Battaglia, Lisa P. Weaver, Ali Zekavat, Mensur Dlakic, Monika Damek Scuron, Patrik Nygrand, & Bruce J. Shenker

DOI: https://dx.doi.org/10.1128/IAI.00788-15

The *Aggregatibacter actinomycetemcomitans* cytolethal distending toxin active subunit, CdtB, contains a cholesterol recognition sequence required for toxin binding and subunit internalization

Kathleen Boesze-Battaglia[a], Lisa P. Walker[b], Ali Zekavat[b], Mensur Dlakić[c], Monika Damek Scuron[b] Patrik Nygren[d] and Bruce J. Shenker[b#]

Departments of Biochemistry[a] and Pathology[b], University of Pennsylvania School of Dental Medicine, Philadelphia, PA USA, Department of Microbiology and Immunology[c] Montana State University, Bozeman, MT USA and the Divisions of Molecular Surface Physics and Nanoscience and Molecular Physics[d], Linköping University, Linköping, Sweden

Running Head: Cytolethal distending toxin subunit B binds to cholesterol

[#]Address correspondence to: Bruce J. Shenker, Ph.D., shenker@upenn.edu

Abstract

Induction of cell cycle arrest in lymphocytes following exposure to the *Aggregatibacter actinomycetemcomitans* cytolethal distending toxin (Cdt) is dependent upon the integrity of lipid membrane microdomains. Moreover, we have previously demonstrated that the associaton of Cdt with target cells involves the CdtC subunit which binds to cholesterol via a cholesterol recognition amino acid consensus sequence (CRAC site). In this study we demonstrate that the active Cdt subunit, CdtB, also is capable of binding to large unilamellar vesicles (LUVs) containing cholesterol. Furthermore, CdtB binding to cholesterol involves a similar CRAC site as that demonstrated for CdtC. Mutation of the CRAC site reduces binding to model membranes as well as toxin binding and CdtB internalization in both Jurkat cells and human macrophages. A concomitant reduction in Cdt-induced toxicity was also noted indicated by reduced cell cycle arrest and apoptosis in Jurkat cells and a reduction in the pro-inflammatory response in macrophages (IL-1β and TNFα release). Collectively, these observations indicate that membrane cholesterol serves as an essential ligand for both CdtC and CdtB and further, that this binding is necessary for both internalization of CdtB and subsequent molecular events leading to intoxication of cells.

Introduction

Aggregatibacter actinomycetemcomitans is a Gram-negative organism that is associated with aggressive forms of periodontitis and other systemic infections (1-5). Periodontitis is a chronic infectious inflammatory disorder that ultimately leads to the destruction of tooth-supporting tissue. While the exact nature of the pathogenesis of periodontal disease and contribution of bacteria to this process is not known, it is becoming increasingly clear that *A. actinomycetemcomitans* produces several potential virulence factors; these include adhesins and fimbria which have been shown to contribute to colonization of the human oral cavity as well as two exotoxins, cytolethal distending toxin (Cdt) and leukotoxin, both of which are capable of killing and/or altering the function of host immune cells (4,6-8).

The Cdts are a family of heat-labile protein cytotoxins produced by several additional bacterial species including *Campylobacter jejuni*, Shigella species, *Haemophilus ducreyi* and diarrheal disease-causing enteropathogens such as some *Escherichia coli* isolates (9-15). There is clear evidence that Cdts are encoded by three genes, designated *cdtA*, *cdtB*, and *cdtC* which are arranged as an apparent operon (7,15-20). The Cdt holotoxin consists of three subunits, CdtA, CdtB and CdtC, that form a heterotrimeric complex. Furthermore, there is considerable agreement among investigators that regardless of the microbial source of Cdt, the heterotrimeric holotoxin functions as an AB_2 toxin where CdtB is the active (A) unit and the complex of CdtA and CdtC comprise the binding (B) unit (18,21,22). Indeed, several investigators have demonstrated that the internalization of CdtB, requires the presence of both CdtA and CdtC (21,23,24).

While several cell types and cell lines have been shown to be susceptible to the toxic actions

of Cdt, tropism for specific cells and/or tissue remains to be identified. In this regard, we have demonstrated that lymphocytes *in vitro* are most susceptible, requiring very low concentrations of Cdt (pg/ml) to induce cell cycle arrest and apoptosis versus other cell types that typically require as much as microgram quantities (25). Typically, susceptibility to bacterial toxins is dependent upon the expression of specific receptors or moieties that enable the toxin to preferentially associate with target host cells. Structural analysis of CdtA and CdtC identified ricin-like lectin domains suggesting that these units interact with cell surface carbohydrate moieties (18). Several investigators have further demonstrated that depending on Cdt source, toxin binding to target cells was dependent upon cell surface N-linked glycoproteins, fucose, glycans or glycosphingolipid (26,27).

In previous studies we have demonstrated that *A. actinomycetemcomitans* Cdt subunits CdtA and CdtC are not only required for the toxin to associate with lymphocytes, but are responsible for localizing the toxin to lipid membrane microdomains (28,29). Furthermore, Cdt-mediated toxicity was found to be dependent upon the integrity of these lipid domains. Previously, we demonstrated that toxin association with lymphocytes, delivery of CdtB to intracellular targets and the induction of both cell cycle arrest and apoptosis was dependent upon cholesterol (29). Specifically, we have shown that the CdtC subunit contains a cholesterol recognition amino acid consensus site (CRAC) that binds to cholesterol in the context of lipid membrane microdomains. More recently, other investigators have also demonstrated CRAC sites on Cdt produced by *H. parasuis* and *C. jejuni* (30,31). We now report that in addition to CdtC, the active subunit CdtB, also contains a CRAC site that is required for its internalization and the induction of toxicity in both lymphocytes and macrophages.

Methods and Materials

Cell culture and analysis for cell cycle and apoptosis.

The human leukemic T cell line, Jurkat (E6-1), was maintained in RPMI-1640 supplemented with 10% FCS, 2 mM glutamine, 10 mM HEPES, 100 U/ml penicillin and 100 µg/ml streptomycin. Cells were harvested in mid-log growth phase and plated at 5 x 10^5 cells/ml, or as indicated, in 24-well tissue culture plates. Cells were exposed to medium, CdtA and CdtC along with $CdtB^{WT}$ or mutants for 18 hr (cell cycle) or 48 hr (apoptosis). To measure Cdt-induced cell cycle arrest, cells were incubated for the time indicated and then washed and fixed for 60 min with cold 80% ethanol (28). The cells were stained with 10 µg/ml propidium iodide containing 1 mg/ml RNase (Sigma Chemical) for 30 min. Samples were analyzed on a Becton-Dickinson LSRII flow cytometer (BD Biosciences) as previously described (28). A minimum of 15,000 events were collected for each sample; cell cycle analysis was performed using Modfit (Verity Software House).

DNA fragmentation in Cdt-treated Jurkat cells was employed to determine the percentage of apoptotic cells using the TUNEL assay [In Situ Cell Death Detection Kit; (Boehringer Mannheim; Indianapolis, IN)]. Jurkat cell cultures were prepared as described above; at the end of the incubation period cells were centrifuged, resuspended in 1 ml of freshly prepared 4% formaldehyde and vortexed gently. After 30 min at RT, the cells were washed with PBS and permeabilized in 0.1% Triton X-100 for 2 min at 4°C. The cells were then washed with PBS and incubated in a solution containing FITC labeled nucleotide and terminal deoxynucleotidyl transferase (TdT) according to the manufacturers specifications. Following the final wash, the cells were resuspended in PBS and analyzed by flow cytometry.

The human acute monocytic leukemia cell line, THP-1, was obtained from ATCC; cells were

maintained in RPMI 1640 containing 10% FBS, 1mM sodium pyruvate, 20 μM 2-mercaptoethanol and 2% penicillin-streptomycin at 37°C with 5% CO_2 in a humidified incubator. THP-1 cells were differentiated into macrophages by incubating cells in the presence of 50 ng/ml PMA for 48 hr at which time the cells were washed and incubated an additional 24 hr in medium prior to use.

Construction and expression of plasmid containing CdtB mutant genes

Amino acid substitutions were introduced into the *cdtB* gene by *in vitro* site-directed mutagenesis using oligonucleotide primer pairs containing appropriate base changes (Table 1). Site-directed mutagenesis was performed using the QuikChange II site-directed mutagenesis kit (Stratagene) according to the manufacturers directions. Amplification of the mutant plasmid was carried out using PfuUltra HF DNA polymerase (Stratagene). All mutant constructs utilized pGEMCdtB as a template; construction and characterization of this plasmid was previously described (28).

In vitro expression of Cdt peptides and CdtB mutants was performed using the Rapid Translation System (RTS 500 ProteoMaster; Roche Applied Science) as previously described (28). Reactions were run according to the manufacturers specification (Roche Applied Science) using 10-15 μg of template DNA. After 20 hrs at 30°C, the reaction mix was removed and the expressed Cdt peptides were purified by nickel affinity chromatography as described (28). Each CdtB peptide contains a His-tag on its C-terminus; previous studies have demonstrated that the presence of the His does not interfere with biological activity (24).

Immunofluorescence and flow cytometry

Jurkat cells or THP-1 derived macrophages (2 x 10^6) were incubated for 30 min (surface staining) or 1 hr (intracellular staining) in the presence of medium or 2 μg/ml of $CdtB^{WT}$ or mutant in the presence of CdtA and CdtC at 37°C (internalization) or 5°C (surface binding). Surface CdtC was detected by washing cells, exposure to normal mouse IgG (Zymed Labs; San Franscisco, CA) and then stained (30 min) for CdtC peptides with anti-CdtC subunit mAb conjugated to AlexaFuor 488 (Molecular Probes; Eugene, OR) according to the manufacturers directions. After washing, the cells were fixed in 2% paraformaldehyde and analyzed by flow cytometry as previously described (29). Intracellular CdtB was detected after exposure of cells to toxin (above) and fixation with 2% formaldehyde for 30 min followed by permeabilization with 0.1% Triton X-100 in 0.1% sodium citrate and stained with anti-CdtB mAb conjugated to Alexafluor 488 (Molecular Probes).

Measurement of cytokine production

Cytokine production was measured in THP-1 derived macrophages (2 x 10^5 cells) incubated for 5 hr. Culture supernatants were collected and analyzed by ELISA for IL-1β (Quantikine Elisa Kit; R and D Systems) and TNFα (Peprotech) using commercially available kits according to the manufacturers instructions. In each instance, the amount of cytokine present in the supernatant was determined using a standard curve.

Preparation of LUVs and Bio-layer Interferometry (BLI)

Phosphatidylcholine (PC), phosphatidylethanolamine-biotin, (PE), phosphatidylserine (PS), sphingomyelin (SM) and cholesterol were obtained from Avanti Polar Lipids; lipids were stored in chloroform at -20ºC with desiccation. Briefly, LUVs were prepared with a lipid ratio of PC/SM/PE

= 50:13:37 (mol %) or as indicated in the presence of varying amounts of cholesterol as previously described by (32,33). For some experiments LUV cholesterol was substituted with stigmasterol as described in the Figure Legends. Lipids were co-solubilized in chloroform, dried under N_2 and trace amounts of residual solvent removed under high vacuum. The lipid mixtures were re-hydrated at a concentration of 8 mM (total phospholipid) in 20 mM Tris-HCl, pH 7.4 containing 50 mM NaCl for 1 hr; the suspensions were then vortexed, freeze-thawed in liquid nitrogen and LUV prepared by extrusion; 11 passes through a 100nm membrane (Mini Extruder; Avanti Polar Lipids).

BLI analyses were performed using a Octet QK^e system (FortéBio) with LUVs comprised of biotinylated-PE immobilized on streptavidin sensors in PBS containing 1 mM n-octyl-β-D-glucopyranoside (OG). Assays were performed in black 96 well plates with a total working volume of 200 µl per well at 30°C with a rpm setting of 1000. Following immobilization of the substrate (LUVs), free streptavidin moieties on the BLI sensors were blocked with biocytin. Measurement of interactions between LUVs and CdtB (and mutants) were performed by incubating the immobilized substrate with varying concentrations of CdtB^{WT} (or mutants) in PBS containing 1 mM OG. CdtB was allowed to associate with LUVs for 10 min followed by a ten min dissociation in binding buffer alone. After subtraction of the signal from a buffer-alone blank sensor, the data were analyzed using Octet Data Analysis software using a 1:1 global fit model to calculate K_D.

Phosphatase assay

Phosphatase activity was assessed by monitoring the dephosphorylation of phosphatidylinositol-3,4,5-triphosphate (PI-3,4,5-P_3) as previously described (25,34). Briefly, the reaction mixture (20 µl) consisted of 100 mM Tris-HCl (pH 8.0), 10 mM dithiothreitol, 0.5 mM

diC16-phosphatidylserine (Avanti), 25 μM PI-3,4,5-P_3 (diC16; Echelon) and the indicated amount of CdtB, CdtABC or PTEN (kindly provided by Gregory Taylor). Appropriate amounts of lipid solutions were deposited in 1.5 ml tubes, organic solvent removed, the buffer added and a lipid suspension formed by sonication. Phosphatase assays were carried out at 37°C for 30 min; the reactions were terminated by the addition of 15 μl of 100 mM N-ethylmaleimide. Inorganic phosphate levels were then measured using a malachite green assay. Malachite green solution (Biomol Green; Biomol) was added to 100 μl of the enzyme reaction mixture and color was developed for 20 min at RT. Absorbance at 650 nm was measured and phosphate release quantified by comparison to inorganic phosphate standards.

Statistical analysis

Mean ± standard error of the mean were calculated for replicate experiments. Significance was determined using a Student's *t*-test; differences between multiple treatments were compared by ANOVA paired with Tukeys HSD posttest; a *P*-value of less than 0.05 was considered to be statistically significant.

Results

It is generally accepted that the association of Cdt holotoxin with target cell membranes involves a binding component comprised of the CdtA and CdtC subunits; moreover, this interaction is required for subsequent delivery of the active subunit, CdtB, to intracellular compartments. We have previously demonstrated that the CdtC subunit contains a CRAC region that is involved in CdtC binding to cholesterol within the plasma membrane as well as to model membranes (33). In addition to CdtC, we have now determined that CdtB also contains a CRAC site: -^{104}*VYIYYSR*^{110}-; the CRAC site conforms to the pattern (L/V)-X_{1-5}-Y-X_{1-5}-(R/K) in which X_{1-5} represents between one and five residues of any amino acid. Figure 1 shows the position (yellow) of the CdtB CRAC site based upon CdtB's crystalized structure; this putative cholesterol binding region is clearly spatially separated from either of the Cdt binding subunits: CdtA and CdtC. Two edges of the site are exposed to the surface while the middle is buried within the structure suggesting that it would not be very accessible. While the CRAC site would appear to have minimal access for binding, there is a loop, (-^{81}IQHGGTPI^{88}-) that is potentially flexible enough to move out of the way and provide access to the CRAC site. Moreover, the hydrophobic stretch of the CRAC site (-^{104}*VYIYY*^{108}-) is compatible with hydrophobic binding that might occur in the context of membrane lipid microdomains. Based upon these molecular models and mutational analysis of critical residues performed on CRAC regions of other proteins, we decided to generate four single-point mutants: CdtB^{V104P}, CdtB^{Y105P}, CdtB^{Y107P} and CdtB^{R110P} to enable us to study the contribution of the CRAC region to toxin interaction with model membranes and host cells.

We previously employed surface plasmon resonance (SPR) to assess the role of the CRAC region within the CdtC subunit and its interaction with cholesterol containing LUVs. In our current

study, Bio-Layer Interferometry (BLI) was employed to assess the CdtB associated CRAC region; BLI is a label-free technology that measures molecular interactions in real time for the purpose of detecting, quantifying and performing kinetic analysis (35). We initially employed the Cdt holotoxin and compared the affinity constant (K_D) obtained with BLI to that previously determined with SPR. Cholesterol-containing LUVs prepared with PE-biotin were immobilized on streptavidin biosensor plates; Cdt holotoxin (0-50 μM) was added to wells and the association and dissociation between toxin and LUV were determined (Fig. S1). The K_D was determined to be 2.03 x 10^{-6} M compared to 3.09 x 10^{-6} M previously determined by SPR (33). We next assessed the binding of the CdtB subunit by adding varying concentrations of $CdtB^{WT}$ (0-50 μM) to wells and the association and dissociation between toxin and LUV were measured over a 10 minute period. Fig. 2A shows a representative series of overlay responses (both real data and modeled data are plotted) for varying concentrations of $CdtB^{WT}$; based on these responses the K_D was calculated to be 1.37±0.2 x 10^{-6} M (Fig. 2E). Previously, we determined that the CdtC subunit binding to LUV was not only cholesterol dependent, but sterol specific as well. Therefore, to determine if CdtB exhibits similar properties to CdtC, LUVs were prepared with 20% cholesterol, 20% stigmasterol or without sterol(33). As shown in Fig. 2D, $CdtB^{WT}$ binding to LUV was sterol dependent and specific; maximum binding to LUV containing cholesterol was 0.24±0.02 nm, a measurement of increased sensor thickness, whereas binding to LUV containing stigmasterol or to LUV prepared without sterol resulted in reduced sensor thickness (binding): 0.12±0.02 nm and 0.04±0.01 nm, respectively.

We next compared the binding affinity of CdtB containing CRAC mutants to wildtype protein. Three of the mutants, $CdtB^{V104P}$, $CdtB^{Y105P}$ and $CdtB^{Y107P}$ exhibited significantly reduced ability to bind to cholesterol containing LUVS; the K_D for $CdtB^{V104P}$ was determined to be 2.08±0.8

x 10^{-5} M while $CdtB^{Y105P}$and $CdtB^{Y107P}$ binding was too weak and the K_D value could not be calculated even when higher protein concentrations were employed (Fig.2B and 2E). In contrast to the these three mutants, a fourth CRAC mutant, $CdtB^{R110P}$, retained its ability to bind to cholesterol containing LUVs; this mutant exhibited an increase in binding with a K_D of 3.35±1.9 x 10^{-8} M (Fig. 2C and 2E). It should be noted that changes in the ability of the CdtB mutant proteins to bind to LUVs was not likely due to alterations in structure; CD analysis of these proteins failed to demonstrate significant differences amongst these mutants relative to $CdtB^{WT}$ (Fig. S2)

In previous studies, we demonstrated that Cdt holotoxin binds to target cells with outcomes that are cell type specific. For example, exposure of lymphocytes to Cdt results in cell cycle arrest and apoptosis; in contrast, toxin-treated macrophages derived from either the human THP-1 cell line or monocytes do not become apoptotic but instead are induced to synthesize and secrete pro-inflammatory cytokines (17,28,36). It should be pointed out that toxin binding to both lymphocytes and macrophages was dependent upon cholesterol and the CRAC region on CdtC. Therefore, we next determined if the CRAC site on CdtB was also important for internalization of this subunit in both lymphocytes and macrophages. Jurkat cells were treated with Cdt subunits as described in *Materials and Methods* and then permeabilized, stained with anti-CdtB mAb conjugated to AlexaFluor 488 and analyzed by flow cytometry. Cells treated with subunits CdtA and CdtC as well as untreated cells served as controls and exhibited minimal fluorescence: mean channel fluorescence (MCF) was 5.7 and 7.2, respectively (Fig 3A). Intracellular CdtB was detected in cells exposed to $CdtB^{WT}$ in the presence of CdtA and CdtC subunits exhibiting a MCF of 24.9 (Fig. 3B). The three CdtB CRAC mutants, $CdtB^{V104P}$, $CdtB^{Y105P}$ and $CdtB^{Y107P}$, which failed to interact with cholesterol containing LUVs also were unable to enter Jurkat cells; MCF was 4.3, 6.1 and 3.6, respectively (Fig.

3C-E). In contrast, cells exposed to the mutant that retained cholesterol binding capability with LUVs, $CdtB^{R110P}$, contained detectable protein [Fig 3F;(MCF=29)]. Pooled results from multiple experiments is shown in Fig. 6A; MCF was reduced to 17.2±0.6% ($CdtB^{V104P}$), 34.1±5.6%($CdtB^{Y105P}$) and 16.9±0.8% ($CdtB^{Y107P}$) of that observed with $CdtB^{WT}$ while $CdtB^{R110P}$ exhibited 104.4±11.7%. Similar results were observed with THP-1 derived macrophages (Fig. 4); control cells and cells exposed to CdtA and CdtC exhibited background fluorescence of 8.6 whereas cells exposed to $CdtB^{WT}$ contained detectable intracellular CdtB (MCF=33.9). CdtB was not detectable in macrophages treated with $CdtB^{V104P}$ (MCF= 8.5), $CdtB^{Y105P}$ (MCF=6.7) and $CdtB^{Y107P}$ (MCF=11.3) while cells treated with $CdtB^{R110P}$ exhibit increased immunofluorescence (MCF=37). As shown in Fig. 6B, results from multiple experiments demonstrate significant reductions in intracellular associated immunofluorescence of 25.4±11.6% ($CdtB^{V104P}$), 28.1±3.8% ($CdtB^{Y105P}$) and 29.1±13.5% of that observed with $CdtB^{WT}$, while $CdtB^{R110P}$ exhibited an increase (144.3±25.1) in fluorescence that was not statistically significant.

We have previously demonstrated that non-cholesterol binding CdtC CRAC mutants prevent toxin binding to target cells (33). Therefore, we wanted to determine if, in addition to preventing internalization, the CdtB CRAC mutants also affected the ability of holotoxin to associate with cells. For these studies, Jurkat cells were treated as described above except that the incubation was performed at 5°C, which we have previously shown blocks CdtB internalization but does not interfere with toxin binding to the cell surface. Cells were then analyzed for the presence of the CdtC subunit on the cell surface as cells were stained without permeabilization. Results are shown in Fig. 5 and demonstrate CdtC was detectable on cells exposed to $CdtB^{WT}$; the MCF was 16.2 (Fig. 5B) versus 5.5 and 5.9 in control cells (Figs. 5A). Cells exposed to Cdt containing either $CdtB^{V104P}$,

CdtB^{Y105P} or CdtB^{Y107P} did not contain detectable CdtC on the surface: MCF was 5.6, 4.6 and 5.9 (Figs. 5D and 5E), respectively. In contrast, cells treated with toxin containing CdtB^{R110P} did contain detectable CdtC on the surface (MCF=12.2). Figure 6C shows pooled results from multiple experiments and demonstrate that the reductions in toxin binding were significant for CdtB^{V104P} (43.5±4.78%), CdtB^{Y105P} (27.8±0.8%) and CdtB^{Y107P} (45.9±5.0%).

It is well established that toxin binding and subsequent internalization of CdtB is required for intoxication of cells (37,38), although the specific intracellular target is somewhat controversial (i.e., nuclear vs cytoplasmic vs membrane). Nonetheless, to corroborate that the three CdtB CRAC mutants were unable to enter target cells, we next assessed their ability to induce toxicity in both lymphocytes and macrophages. The effect of CdtB mutants on Jurkat cell cycle arrest is shown in Fig. 7. Cells exposed to medium alone exhibited 9% G2 cells. In contrast, cells treated with CdtB^{WT} exhibited an increasing percent of G2 cells as the dose of toxin was incremented: 21% (0.8 ng/ml CdtB^{WT}), 29% (4.0 ng/ml CdtB^{WT}) and 42% (20 ng/ml CdtB^{WT}). Likewise, cells treated with the same doses of toxin comprised of CdtB^{R110P} also exhibited increases in the percentage of G2 cells: 11%, 17% and 26%, respectively. However, Jurkat cells treated with CdtB^{V104P}, CdtB^{Y105P}, or CdtB^{Y107P} failed to exhibit cell cycle arrest as the percentage of G2 cells was similar to that observed in control cells regardless of protein concentration.

In addition to cell cycle, toxin treated Jurkat cells were assessed for apoptosis using the TUNEL assay 48 hr following exposure to the same protein concentrations utilized for cell cycle. Control cells (medium only) as well as cell cultures exposed to the CdtA and CdtC subunits only exhibited 19 % apoptosis. As shown in Fig. 8, Jurkat cells treated with CdtB^{WT} exhibited dose dependent increases in the percentage of apoptotic cells: 42.±13.9 (4 ng/ml CdtB) and 53.1±10.2 (20

ng/ml CdtB). The CRAC mutant that retained the ability to bind to cholesterol containing LUVs, $CdtB^{R110P}$, also retained the ability to induce Jurkat cell apoptosis; exposure to this mutant resulted in 25.6±9.2 (4 ng/ml) and 41.6±11.4 % apoptotic cells. In contrast, treatment of lymphocytes with either of the non-cholesterol binding CdtB CRAC mutants (0.4-20 ng/ml), $CdtB^{V104P}$, $CdtB^{Y105P}$ or $CdtB^{Y107P}$, failed to result in apoptosis.

In previous studies, we have identified macrophages as another potential target of Cdt (36). However, macrophages derived from either human blood monocytes or the monocytic leukemic cell line, THP-1, were not susceptible to Cdt-induced apoptosis. Instead, Cdt induced a pro-inflammatory cytokine response in these cells within 2 hr. Moreover, toxin interaction with these cells was shown to be cholesterol dependent as toxin comprised of CdtC containing a CRAC mutant failed to bind to macrophages and were unable to induce cytokine synthesis and release. Therefore, we also assessed the ability of CdtB-containing CRAC mutants to induce a pro-inflammatory cytokine response in THP-1 derived macrophges. As shown in Fig. 9, treatment of macrophages with $CdtB^{WT}$ resulted in increased release of IL-1β; control cells produced 24.6±1.3 pg/ml while exposure to 20 ng/ml CdtB resulted in 336.4±29.3 pg/ml IL-1β. Similar results were obtained for TNFα; control cells released 168.2±17.9 pg/ml and cells exposed to 20 ng/ml CdtB induced the release of 1676.8± 261.0 pg/ml TNFα. Treatment of macrophages with $CdtB^{V104P}$, $CdtB^{Y105P}$ or $CdtB^{Y107P}$ resulted in a significantly lower cytokine response in comparison to that observed with $CdtB^{WT}$: 83.9±12.0 pg/ml IL-1β and 481±125.7 pg/ml TNFα in the presence of $CdtB^{V104P}$, 86.6±14.7 pg/ml IL-1β and 477.1±74.6 pg/ml TNFα in the presence of $CdtB^{Y105P}$ and 96.2±7.5 pg/ml IL-1β and 486.2±88.3 pg/ml TNFα in the presence of $CdtB^{Y107P}$. Although these values are significantly lower than that observed with $CdtB^{WT}$, they do represent increases over background levels suggesting the

the mutants retained residual low level binding. Macrophages exposed to $CdtB^{R110P}$ exhibited a robust dose-dependent cytokine response relative to the other two CdtB mutants but somewhat less than that observed with $CdtB^{WT}$: 216.0±11.9 pg/ml IL-1β and 1091.4±117.6 pg/ml TNFα; these differences were not statistically different from those values obtained with $CdtB^{WT}$.

In previous studies we have demonstrated that Cdt-induced toxicity in lymphocytes (cell cycle arrest and apoptosis) and macrophages (pro-inflammatory cytokine response) were dependent upon CdtB's ability to function as a PIP3 phosphatase (25,36). Therefore, we next confirmed that our observations regarding the loss of toxicity associated with the CdtB CRAC mutants was not due to altered phosphatase activity. $CdtB^{WT}$ was initially assessed for its ability to dephosphorylate PI-3,4,5-$P_{3;}$ as shown in Fig 10, the wildtype subunit exhibits dose-dependent phosphate release: 0.24±0.04, 0.73±0.20 and 1.39±0.34 nmol/30 min in the presence of 0.25, 0.5 and 1.0 μM CdtB, respectively. All four CdtB mutants exhibited similar activity that was slightly, but not significantly lower than that observed with $CdtB^{WT}$. In the presence of 0.5 μM protein, phosphatase release was 0.42±0.17 ($CdtB^{V104P}$), 0.43±0.3 ($CdtB^{Y105P}$), 0.50±0.28 ($CdtB^{Y107P}$) and 0.52±0.22 nmol ($CdtB^{R110P}$); phosphatase activity increased in the presence of 1.0 μM protein to 0.94±0.21 ($CdtB^{V104P}$), 0.94±0.25 ($CdtB^{Y105P}$), 1.12±0.20 ($CdtB^{Y107P}$) and 1.01±0.21 nmol ($CdtB^{R110P}$).

Discussion

It is generally accepted that all three Cdt subunits, CdtA, CdtB and CdtC, are required to achieve maximal toxic activity, regardless of the target cell. Thus, the holotoxin is believed to function as an AB2 toxin where the cell binding unit, B, is responsible for toxin binding to the cell surface and thereby deliver the active subunit, A, to intracellular compartments. In the context of Cdt, binding activity is considered to be the result of cooperative activities of both the CdtA and CdtC subunits (reviewed in (39)). Moreover it has been proposed that these subunits share structural homology with lectin-like proteins and further, that fucose moieties might be involved in toxin association with the cell surface(18,26). In other studies, glycosphingolipids have been implicated as possible binding sites as inhibitors of glycosphingolipid synthesis reduce toxin intoxication (27). It should be pointed out that in a more recent study in which Cdts from different microbial species were studied simultaneously, fucosylated structures as well as N- and O-glycans were found not to be required for Cdt-host cell interaction (40). In contrast, these authors observed that Cdt derived from three sources: *A. actinomycetemcomitans*, *C. jejuni* and *H. ducreyi*, were each dependent upon membrane cholesterol thereby confirming the previous observations of Boesze-Battaglia *et al* (33) and Guerra *et al* (37) and more recently those of Zhou *et al* (30) and Lai *et al* (31). These studies are opposed by other investigators who have reported that cholesterol depletion failed to alter toxin subunit internalization (41). It should be noted that this later study is difficult to assess with respect to the role of cholesterol as the experimental protocol utilized a long exposure time to methyl-β-cyclodextrin and further, cholesterol repletion was not employed to demonstrate specificity.

We have previously demonstrated that the Cdt holotoxin co-localizes on the cell surface with

GM1 in the context of cholesterol rich membrane microdomains, or lipid rafts (29). Furthermore, disruption of lipid rafts by cholesterol depletion reduced toxin binding, CdtB internalization and cell susceptibility to Cdt intoxication (33). We have also demonstrated cholesterol specific binding of Cdt to both model membranes and lymphocyte membranes; furthermore, this binding is dependent upon a cholesterol recognition sequence within the CdtC subunit. In this regard, numerous proteins have been shown to bind cholesterol; these include the benzodiazepine receptor, the HIV transmembrane protein gp41, caveolin, G-protein coupled receptors, components of Ca^{++}- and voltage-gated K^+ channels, apolipoproteins, the translocator protein, TSPO and more recently, the leukotoxin produced by *A. actinomycetemcomitans* (42-50). Each of these cholesterol binding proteins contain a CRAC sequence: -L/V-(X)(1-5)-Y-(X)(1-5)-R/K- where (X)(1-5) represents one to five residues of any amino acid. Indeed, we have shown that the CdtC subunit of *A. actinomycetemcomitans* Cdt also contains such a CRAC site: -^{68}LIDYKGK^{74}-; mutation of residues within this region reduced both toxin binding to LUVs and cells, CdtB internalization and toxicity. In the current study we have analyzed the active subunit of the *A. actinomycetemcomitans* Cdt, CdtB, for its ability to bind to LUVs containing cholesterol. Indeed, CdtB^{WT} not only demonstrates high affinity for cholesterol containing LUVs, but binding was significantly reduced when LUVs either did not contain any sterol or stigmasterol was utilized as a substitute for cholesterol. These observations led us to consider the possibility that like CdtC, CdtB also might contain a CRAC site; indeed motif analysis of CdtB confirmed the presence of a CRAC site: -^{104}*VYIYYSR*^{110}-.

In order to study the requirement for the CdtB CRAC site in binding to LUVs and cells, we mutated four residues within this site (shown in bold), -^{104}***VYIYYSR***^{110}-; we predicted three of these would be critical to its binding function . First, CdtB^{V104P} CdtB^{Y107P} were selected because they

represent critical residues within the CRAC motif. Also, they are very well conserved in all CdtB proteins with the exception of $CdtB^{V104}$ which is not conserved in toxin from bacteria that are facultative intracellular pathogens such as Salmonella. Thus, Salmonella-derived CdtB most likely utilize a different pathway to reach their intracellular target as opposed to that used by CdtB produced by bacteria that are associated with extracellular infection such as *A. actinomycetemcomitans*. This raises the likelihood that $CdtB^{V104P}$ is a critical residue for cholesterol interaction since it is unlikely that the Salmonella-derived toxin is dependent upon a pathway that has a requirement for binding to plasma membrane cholesterol. Second, $CdtB^{Y105P}$ and $CdtB^{Y107P}$ were selected as they are among the most conserved residues in the entire CRAC site and therefore, there was a high likelihood that they would be critical to the function of the CRAC site. Finally, $CdtB^{R110P}$ was selected as this is the least conserved CRAC residue amongst the CdtB proteins. In fact, several CdtB proteins from Helicobacter species have a proline conserved at this position instead of arginine. Therefore, we expected that not only was this residue not critical to CRAC function, but that the proline substitution would also not contribute to any change in cholesterol binding. Thus $CdtB^{R110P}$ served as a control for the other mutations.

Analysis of the $CdtB^{V104P}$, $CdtB^{Y105P}$ and $CdtB^{Y107P}$ mutants demonstrate reduced ability to bind to LUVs as well as decreased internalization in both lymphocytes and macrophages. Moreover, analysis of the effect of CdtB CRAC mutants on Cdt holotoxin binding to the cell surface indicated that these CdtB mutations did not permit holotoxin association with target cells as well. These observations are consistent with our previous studies involving mutation of the CRAC region within CdtC (33) and those of other investigators who made similar CRAC mutations of residues within the CdtC subunit of Cdts produced by other bacterial species as well as to other cholesterol binding

proteins (30,31,42,50). In each instance CRAC mutations resulted in a loss of cholesterol binding and associated downstream biological effects; in contrast, $CdtB^{R110P}$, had no effect on Cdt binding and CdtB internalization confirming our expectation for the relative role of each of these residues within the CRAC site and overall role in CdtB-cholesterol interaction. It should be noted that we don't have a clear explanation for the observed increase in affinity for this mutant.

The CRAC domain is a short linear motif that is in the N-terminus to C-terminus direction and represents the most popular cholesterol-binding domain. More recently, Baier et al (51) identified another cholesterol-binding motif, CARC, with a sequence similar to that of CRAC but oriented in along the polypeptide chain in the opposite direction. CARC constitutes an inverted CRAC domain: (K/R)-X_{1-5}-(Y/F)-X_{1-5}-(L/V) from the N-terminus to the C-terminus. Interestingly, we found that a CARC site exists in CdtB and is embedded within the CRAC site (shown in bold): -^{100}RPNM**VYIYYSR**L^{111}-. While we can not entirely exclude the possibility that the CARC motif may also contribute to CdtB-cholesterol binding, we believe that the analysis of the CRAC mutants is more consistent with a functional role for the CRAC motif. Furthermore, $CdtB^{R100}$ is only moderately conserved amongst CdtB proteins.

The location of the CRAC site based upon molecular models of the crystalized structure of CdtB indicates that the region has two exposed edges and a buried middle region. Our mutation analysis suggests that the lower region (Fig. 1) and buried middle region are critical to binding. These results would suggest that the structure of CdtB, and availability of the CRAC site, is likely altered in the context of lipid rafts as opposed to the rigid crystal structure.

It should also be noted that in previous studies we demonstrated that depletion of cholesterol from lymphocyte membranes reduced Cdt holotoxin binding, CdtB internalization and toxicity (33).

Likewise, repletion studies in which membrane cholesterol was restored also resulted in re-establishment of toxin binding, CdtB internalization and susceptibility to Cdt intoxication. We initially interpreted these results as evidence for the role of cholesterol and the CdtC CRAC site in toxin-cell interactions; however, it should now be noted that these observations are also consistent with our current findings for a critical role for cholesterol and the CdtB CRAC site as well.

Finally, we assessed the CdtB CRAC mutants for their ability to intoxicate cells. For these studies we employed two host target cells: lymphocyte and macrophages. Jurkat cells treated with the three CdtB cholesterol-binding defective mutants, $CdtB^{V104P}$, $CdtB^{Y105P}$ and $CdtB^{Y107P}$, also exhibited reduced toxicity which was reflected in fewer cells in G2 arrest at 18 hr and less apoptotic cells at 48 hr relative to $CdtB^{WT}$. Likewise, the pro-inflammatory cytokine response that is induced in macrophages treated with wildtype toxin was reduced in cells treated with the defective cholesterol binding mutants; this was reflected in reduced secretion of both IL-1β and TNFα. The fourth CRAC mutant, $CdtB^{R110P}$, was unaltered in its ability to bind to cholesterol containing LUVs and to deliver CdtB to intracellular compartments in both Jurkat cells and macrophages. Likewise, the $CdtB^{R110P}$ mutant exhibited toxic activity comparable to $CdtB^{WT}$ as it induced both G2 arrest and apoptosis in lymphocytes and cytokine release in macrophages. While $CdtB^{R110P}$ was able to bind, internalize and intoxicate cells, the latter was less than that observed with $CdtB^{WT}$, although these differences were not statistically significant.

In previous studies we demonstrated that toxic effects of Cdt on both lymphocytes and macrophages were dependent upon the ability of CdtB to function as a phosphatidylinositol-3,4,5-triphosphate phosphatase (25,36). Thus, we also assessed the CdtB mutants for lipid phosphatase activity; indeed, all three CdtB CRAC mutants retained enzymatic activity at levels comparable to

the wildtype protein. This finding provides further evidence that reduced toxicity associated with these mutants is the result of changes in cell binding and internalization rather than altered structure and/or molecular mode of action associated with the active subunit; the former was confirmed by CD analysis.

Collectively, our current findings, along with previous observations, provide strong support for the notion that Cdt association with target cells is dependent upon both the CdtC and CdtB subunits ability to bind to cholesterol. Furthermore, our observations demonstrate that Cdt-host cell association involves membrane microdomains enriched in cholesterol and is dependent upon the integrity of these so-called lipid rafts. Lipid rafts represent liquid-ordered microdomains which are distributed in the plasma membrane and whose lipid composition and high cholesterol content differs from the rest of the membrane (52). Generally, lipid rafts are regarded as scaffolds for a number of molecular entities which include ion channels, receptors and signaling platforms; thus these membrane regions provide an ideal structure to facilitate communication of extracellular stimuli to the intracellular milieu leading to signaling events that regulate cell growth, proliferation and survival (53,54).

It is becoming increasingly evident that membrane rafts facilitate target cell interaction with several microbial toxins (55,56); in addition to binding and clustering, these interactions may contribute to toxin internalization and/or molecular mode of action. For instance, lipid membrane rafts may provide a mechanism by which receptors are concentrated and thereby promote ligand or pathogen binding. One such example is cholera toxin which is pentameric and binds to targets cells via the ganglioside GM1. It is likely that cholera toxin simultaneously binds with high affinity to multiple receptors as a result of receptor concentration within the raft (56,57). Likewise, the

pore-forming leukotoxin from *A. actinomycetemcomitans* recognizes cholesterol via a CRAC site which facilitates clustering to its receptor in the context of lipid rafts (50). Another pore forming toxin, the aerolysin from *Aeromonas hydrophila*, which binds to GPI-anchored proteins, also utilize the concentrating properties of rafts to facilitate oligomerization, a requisite for channel formation (56,58). These findings are consistent with the high cholesterol content of lipid rafts which we propose facilitate Cdt binding as well.

Association with lipid rafts may also provide access to endocytic processes and intracellular trafficking routes. For example, Shiga toxin and cholera toxin bind to glycosphingolipids which results in lipid clustering and changes in membrane properties that facilitate internalization and endocytic uptake (59). Likewise, several pathogens enter host cells in a cholesterol-dependent manner (55,56); for example, the uptake of *E. coli* strains which express FimH have been shown to involve cholesterol-rich rafts. Similarly, Shigella invades cells via interaction between the invasin, IpaB, and the raft associated receptor, CD44 (60). Several enveloped and non-enveloped viruses (for example, SV40, HIV and HSV) also require lipid rafts for binding or entry by endocytosis (60). It is interesting to note that not only does Cdt associate with cholesterol in the context of lipid rafts, several investigators have demonstrated that CdtB is internalized by endocytic mechanisms and in the case of *H. ducreyi* Cdt, this appears to be dynamin dependent (38). The latter observation is critical as disruption of the cholesterol binding CRAC region for baculovirus has also been shown to compromise dynamin dependent viral endocytosis (61).

In conclusion, we propose that binding of cholesterol by the CRAC regions contained within the CdtC and CdtB subunits results in the association of the Cdt holotoxin with membrane lipid rafts. It is likely that lipid raft association is critical for not only holotoxin binding, but also the

internalization and, possibly, the function of the active subunit, CdtB. These studies predict that cholesterol disposition within the membrane influences binding of CdtC and CdtB to the cell surface; therefore, we propose that Cdt favors raft associated cholesterol resulting in localized toxin-rich regions. This association may also be critical to the mode of action of the toxin thereby allowing it to hijack lipid raft associated signaling platform(s) and perhaps, provide access to intracellular pools of PI-3,4,5-P_3. Furthermore, perturbation of signaling cascades likely contributes to cell cycle arrest and eventual cell death in lymphocytes; similar events likely contribute to the toxin-induced pro-inflammatory cytokine response in macrophages as well. While these studies do not exclude the possibility of the existence of additional receptors that might be recognized by CdtA, they do clearly demonstrate that cholesterol recognition via CRAC sites and mutation of these regions is sufficient to block Cdt-mediated toxicity in target cells.

Acknowledgments

The authors wish to acknowledge the expertise of the SDM Flow Cytometry Facility in helping carry out this study. This work was supported by the National Institutes of Health grants DE06014 and DE023071.

References

1. **Zambon, J. J.** 1985. *Actinobacillus actinomycetemcomitans* in human periodontal disease. J.Clin.Periodontol. **12**:1-20.

2. **van Winkelhoff, A. and J. Slots**. 1999. *Actinobacillus actinomycetemcomitans* and *Porphyromonas gingivalis* in non oral infections. Periodontol **20**:122-135.

3. **Fine, D., J. Kaplan, S. Kachlany, and H. Schreiner**. 2006. How we got attached to *Actinobacillus actinomycetemcomitans*: a model for infectious diseases. Periodontology 2000 **42**:114-157.

4. **Henderson, B., J. Ward, and D. Ready**. 2010. *Aggregatibacter (Actinobacillus) actinomycetemcomitans*: a triple A* periodontopathogen? Periodontology 2000 **54**:78-105.

5. **Rahamat_Langendoen, J., M. van Vonderen, L. Engstrom, W. Manson, A. van Winkelhoff, and E. Mooi-Kokenberg**. 2011. Brain abscess associated with *Aggregatibacter actinomycetemcomitans*: case report and review of literature. J Clin Perio **38**:702-706.

6. **Rabie, G., E. T. Lally, and B. J. Shenker**. 1988. Immunosuppressive properties of *Actinobacillus actinomycetemcomitans* leukotoxin. Infect.Immun. **56**:122-127.

7. **Shenker, B. J., T. L. McKay, S. Datar, M. Miller, R. Chowhan, and D. R. Demuth**. 1999. *Actinobacillus actinomycetemcomitans* immunosuppressive protein is a member of the family of cytolethal distending toxins capable of causing a G2 arrest in human T cells. J.Immunol. **162**:4773-4780.

8. **Korostoff, J., N. Yamaguchi, M. Miller, I. Kieba, and E. Lally**. 2000. Perturbation of mitochondrial structure and function plays a central role in *Actinobacillus actinomycetemcomitans*

leukotoxin-induced apoptosis. Microb.Pathog. **29**:267-278.

9. **Comayras, C., C. Tasca, S. Y. Peres, B. Ducommun, E. Oswald, and J. De Rycke**. 1997. *Escherichia coli* cytolethal distending toxin blocks the HeLa cell cycle at the G2/M transition by preventing cdc2 protein kinase dephosphorylation and activation. Infection and Immunity **65**:5088-5095.

10. **Okuda, J., M. Fukumoto, Y. Takeda, and M. Nishibuchi**. 1997. Examination of diarrheagenicity of cytolethal distending toxin: suckling mouse response to the products of the cdtABC genes of *Shigella dysenteriae*. Infection and Immunity **65**:428-433.

11. **Okuda, J., H. Kurazono, and Y. Takeda**. 1995. Distribution of the cytolethal distending toxin A gene (cdtA) among species of Shigella and Vibrio, and cloning and sequencing of the cdt gene from *Shigella dysenteriae*. Microb.Pathog. **18**:167-172.

12. **Scott, D. A. and J. B. Kaper**. 1994. Cloning and sequencing of the genes encoding *Escherichia coli* cytolethal distending toxin. Infect.Immun. **62**:244-251.

13. **Pickett, C. L., D. L. Cottle, E. C. Pesci, and G. Bikah**. 1994. Cloning, sequencing, and expression of the Escherichia coli cytolethal distending toxin genes. Infection and Immunity **62**:1046-1051.

14. **Mayer, M., L. Bueno, E. Hansen, and J. M. DiRienzo**. 1999. Identification of a cytolethal distending toxin gene locus and features of a virulence-associated region in *Actinobacillus actinomycetemcomitans*. Infect.Immun. **67**:1227-1237.

15. **Pickett, C. L. and C. A. Whitehouse**. 1999. The cytolethal distending toxin family. Trends in Microbiology **7**:292-297.

16. **Shenker, B. J., R. H. Hoffmaster, T. L. McKay, and D. R. Demuth**. 2000. Expression of

the cytolethal distending toxin (Cdt) operon in *Actinobacillus actinoimycetemcomitans*: evidence that the CdtB protein is responsible for G2 arrest of the cell cyclein human T-cells. J.Immunol **165**:2612-2618.

17. **Shenker, B. J., R. H. Hoffmaster, A. Zekavat, N. Yamguchi, E. T. Lally, and D. R. Demuth**. 2001. Induction of apoptosis in human T cells by *Actinobacillus actinomycetemcomitans* cytolethal distending toxin is a consequence of G_2 arrest of the cell cycle. J.Immunol. **167**:435-441.

18. **Nesic, D., Y. Hsu, and C. E. Stebbins**. 2004. Assembly and function of a bacterial genotoxin. Nature **429**:429-433.

19. **De Rycke, J. and E. Oswald**. 2001. Cytolethal distending toxin (CDT): a bacterial weapon to control host cell proliferaton? FEMS Microbiol.Lett. **203**:141-148.

20. **Thelastam, M. and T. Frisan**. 2004. Cytolethal distending toxins. Rev.Physiol.Biochem.Pharmacol. **152**:111-133.

21. **Lara-Tejero, M. and J. E. Galan**. 2001. CdtA, CdtB, and CdtC form a tripartite complex that is required for cytolethal distending toxin activity. Infect.Immun. **69**:4358-4365.

22. **Elwell, C. A., K. Chao, K. Patel, and L. A. Dreyfus**. 2001. *Escherichia coli* CdtB mediates cytolethal distending toxin cell cycle arrest. Infect.Immun. **69**:3418-3422.

23. **Mao, X. and J. M. DiRienzo**. 2002. Functional studies of the recombinant subunits of a cytolethal distending toxin. Cell.Microbiol. **4**:245-255.

24. **Shenker, B. J., D. Besack, T. L. McKay, L. Pankoski, A. Zekavat, and D. R. Demuth**. 2004. *Actinobacillus actinomycetemcomitans* cytolethal distending toxin (Cdt): evidence that the holotoxin is composed of three subunits: CdtA, CdtB, and CdtC. J.Immunol. **172**:410-417.

25. **Shenker, B. J., M. Dlakic, L. Walker, D. Besack, E. Jaffe, E. Labelle, and K. Boesze-**

Battaglia. 2007. A novel mode of action for a microbial-derived immunotoxin: the cytolethal distending toxin subunit B exhibits phosphatidylinositol (3,4,5) tri-phosphate phospatase activity. J.Immunol. **178**:5099-5108.

26. **McSweeney, L. and L. A. Dreyfus**. 2005. Carbohydrate-binding specificity of the *Escherichia coli* cytolethal distending toxin CdtA-II and CdtC-II subunits. Infect.Immun. **73**:2051-2060.

27. **Mise, K., S. Akifusa, S. Watarai, T. Ansai, T. Nishihara, and T. Takehara**. 2005. Involvement of ganglioside GM3 in G2/M cell cycle arrest of human monocytic cells induced by *Actinobacillus actinomycetemcomitans* cyytolethal distending toxin. Infect.Immun. **73**:4846-4852.

28. **Shenker, B. J., D. Besack, T. L. McKay, L. Pankoski, A. Zekavat, and D. R. Demuth**. 2005. Induction of cell cycle arrest in lymphocytes by *Actinobacillus actinomycetemcomitans* cytolethal distending toxin requires three subunits for maximum activity. J.Immunol. **174**:2228-2234.

29. **Boesze-Battaglia, K., D. Besack, T. L. McKay, A. Zekavat, L. Otis, K. Jordan-Sciutto, and B. J. Shenker**. 2006. Cholesterol-rich membrane microdomains mediate cell cycle arrest induced by *Actinobacillus actinomycetemcomitans* cytolethal distending toxin. Cellular Microbiology **8**:823-836.

30. **Zhou, M., Q. Zhang, J. Zhao, and M. Jin**. 2012. *Haemophilus parasuis* endcodes two functional cytolethal distending toxins: CdtC contains an aytpical cholesterol recognition/interaction region. PLoS ONE **7**:e32580.

31. **Lai, C., C. Lai, Y. Lin, C. Hung, C. Chu, C. Feng, C. Chang, and H. Su**. 2013. Characterization of putative cholesterol recognition/interaction amino acid consensus-like motif of

Campylobacter jejuni cytolethal distending toxin C. PLoS ONE **8**:e66202.

32. **Hekman, M., H. Hamm, A. Villar, B. Bader, J. Kuhlmann, J. Nickel, and U. R. Rapp**. 2002. Associations of B- and C-raf with cholesterol, phosphatidylserine, and lipid second messengers. J.Biol.Chem. **277**:24090-24102.

33. **Boesze-Battaglia, K., A. Brown, L. Walker, D. Besack, A. Zekavat, S. Wrenn, C. Krummenacher, and B. J. Shenker**. 2009. Cytolethal distending toxin-induced cell cycle arrest of lymphocytes is dependent upon recognition and binding to cholesterol. J Biol Chem **284**:10650-10658.

34. **Maehama, T., G. Taylor, J. Slama, and J. Dixon**. 2000. A sensitive assay for phosphoinositide phosphatases. Analytical Biochemistry **279**:248-250.

35. **Wijeyesakere, S., S. Rizvi, and Raghavan**. 2013. Glycan-dependent and -independent interactions contribute to cellular substrate recruitment by calreticulin. J.Biol.Chem. **288**:35104-35116.

36. **Shenker, B., L. Walker, A. Zekavat, M. Dlakic, and K. Boesze-Battaglia**. 2014. Blockade of the PI-3K signaling pathway by the *Aggregatibacter actinomycetemcomitans* cytolethal distending toxin induces macrophages to synthesize and secrete pro-inflammatory cytokines. Cellular Microbiology **16** :1391-1404.

37. **Guerra, L., K. Teter, B. Lilley, B. Stenerlow, R. Holmes, H. Ploegh, J. A. Sandvik, M. Thelastam, and T. Frisan**. 2005. Cellular internalization of cytolethal distending toxin: a new end to a known pathway. Cellular Microbiology **7**:921-934.

38. **Cortes-Bratti, X., E. Chaves-Olarte, T. Lagergard, and M. Thelastam**. 2000. Cellular internalization of cytolethal distending toxin from *Haemophilus ducreyi*. Infect.Immun. **68**:6903-

6911.

39. **Gargi, A., M. Reno, and S. Blanke**. 2012. Bacterial toxin modulation of the eukaryotic cell cycle: are all cytolethal distending toxins created equally. Frontiers in Cellular and Infection Microbiology **2**:124.

40. **Eshraghi, A., F. Maldonado-Arocho, A. Gargi, M. Cardwell, M. Prouty, S. Blanke, and K. Bradley**. 2010. Cytolethal distending toxin family members are differentially affected by alterations in host glycans and membrane cholesterol. J Bio Chem **285**:18199-18207.

41. **Damek-Poprawa, M., J. Jang, A. Volgina, J. Korostoff, and J. DiRienzo**. 2012. Localization of *Aggregatibacter actinomycetemcomitans* cytolethal distending toxin subunits during intoxication of live cells. Infect.Immun. **80**:2761-2770.

42. **Jamin, N., J. Neumann, M. Ostuni, T. Vu, Z. Yao, S. Murail, J. Robert, C. Fiatzakis, V. Papadopoulos, and J. Lacapere**. 2005. Characterization of the cholesterol recognition amino acid consensus sequence of the peripheral-type benzodiazepine receptor. Molecular Endocrin **19**:588-594.

43. **Li, H. and V. Papadopoulos**. 1998. Peripheral-type benzodiazepine receptor function in cholesterol transport. Identification of a putative cholesterol recognition/interaction amino acid sequence and consensus pattern. Endocrinology **139**:4991-4997.

44. **Epand, R., B. Sayer, and R. Epand**. 2005. Caveolin scaffolding region and cholesterol-rich domains in membranes. Journal of Molecular Biology **345**:339-350.

45. **Vincent, N., C. Genin, and E. Malvoisin**. 2002. Identificaton of a conserved domain of the HIV-1 transmembrane protein gp41 which interacts with cholesteyl groups. Biochim.Biophys.Acta **1567**:157-164.

46. **Oddi, S., E. Dainese, F. Fezza, M. Lanuti, D. Barcaroli, V. DeLaurenzi, D. Centonze, and M. Maccarrone**. 2011. Functional characterization of putative cholesterol binding sequence (CRAC) in human type-1 cannabinoid receptor. Journal of Neurochemistry **116**:858-865.

47. **Singh, A., J. McMillan, A. Bukiya, B. Burton, A. Parrill, and A. Dopico**. 2012. Multiple cholesterol recognition/interaction amino acid consensus (CRAC) motifs in cytosolic C tail of Slo1 subunit determine cholesterol sensitivity of Ca^{2+}- and voltage-gated K^{+} (BK) channels. J.Biol.Chem. **287**:20509-20521.

48. **Lecanu, L., Z. Yao, A. McCourty, E. Sidahmed, M. Orellana, M. Burnier, and V. Papadopoulos**. 2013. Control of hypercholesterolemia and atherosclerosis using the cholesterol recognition/interaction amino acid sequence of the translocator protein TSPO. Steroids **78**:137-146.

49. **Jafurulla, M., S. Tiwari, and A. Chattopadhyay**. 2011. Identification of cholesterol recognition amino acid consensus (CRAC) motif in G-protein coupled receptors. Biochem Biophys Res Commun **404**:569-573.

50. **Brown, A., N. Balashova, R. Epand, R. Epand, A. Bragin, S. Kachlany, M. Walters, Y. Du, K. Boesze-Battaglia, and E. Lally**. 2013. *Aggregatibacter actinomycetemcomitans* leukotoxin utilizes a cholesterol recognition amino acid consensus site for membrane association. J.Biol.Chem. **288**:23607-23621.

51. **Baier, C., J. Fantini, and F. Barrantes**. 2011. Disclosure of cholesterol recognition motifs in transmembrane domains of the human nicotinic acetylcholine receptor. Scientific Reports **1**:DOI:10.1038/srep00069.

52. **Head, B., H. Patel, and P. Insel**. 2014. Interaction of membrane/lipid rafts with the cytoskeleton: impact on signaling and function. Biochim Biophys Acta **1838**:532-545.

53. **Dykstra, M., A. Cherukuri, H. Sohn, S. Tzeng, and S. Pierce**. 2003. Location is everything: lipid rafts and immune cell signaling. Annu.Rev.Immunol. **21**:457-481.

54. **Cherukuri, A., M. Dykstra, and S. Pierce**. 2001. Floating the raft hypothesis: lipid rafts play a role in immune cell function. Immunity **14**:657-660.

55. **Lencer, W.** 2001. Microbes and microbial toxins: paradigms for microbial-mucosal interactions *V. cholera*: invasion of the intestinal epithelial barrier by a stably folded protein toxin. Am J Physiol Gastrointest Liver Physiol **280**:G781-G786.

56. **van der Goot, F. g. and T. Harder**. 2001. Raft membrane domains: from a liquid-ordered membrane phase to site of pathogen attack. Seminars in Immunology **13**:89-97.

57. **Montecucco, C., E. Papini, and G. Schiavo**. 1994. Bacterial protein toxins pentrate cells via a four-step mechanism. FEBS Lett. **3466**:92-98.

58. **Abrami, L. and F. g. van der Goot**. 1999. Plasma membrane microdomains act as concentration platforms to facilitate intoxication by aerolysin. J.Cell Biol. **147**:175-184.

59. **Ewers, H. and A. Helenius**. 2011. Lipid-mediated endocytosis. Cold Spring Harb Perspect Biol **3:a004721**.

60. **Lafont, F., G. Tran Van Nhieu, K. Hanada, P. Sansonetti, and F. g. van der Goot**. 2002. Initial steps of *Shigella* infection depend on the cholesterol/sphingolipid raft-mediated CD44-IpaB interaction. EMBO J. **21**:4449-4457.

61. **Luz-Madrigal, A., A. Asanov, A. Camacho-Zarco, A. Sampieri, and L. Vaca**. 2013. A cholesterol recognition aminoi acid consensus domain in GP64 fusion protein facilitatrs anchoring of aculovirus to mammalian cells. Journal of Virology **87**:11894-11907.

Figure Legends:

Figure 1 Localization of the CRAC sites on Cdt. A surface representation of Cdt holotoxin is shown indicating the accessibility of the CdtB CRAC site (yellow) and CdtC CRAC site (white). CdtA is shown in green, CdtC in blue and CdtB in red.

Figure 2 CdtB binding to LUVs containing cholesterol is dependent upon the CRAC site. LUVs containing PE-biotin were immobilized on streptavidin sensors and $CdtB^{WT}$ or CdtB CRAC-containing mutants served as the analyte. Panels A-C show a representative BLI sensorgram for the interaction of varying concentrations of $CdtB^{WT}$, $CdtB^{Y104P}$ and $CdtB^{R110P}$ with LUVs containing 20% cholesterol; the experimental line (black) is shown along with the model fit (red line). Panel D shows the relative binding of 25 μM $CdtB^{WT}$ to LUVs containing 20% cholesterol, 20% stigmasterol or 0% cholesterol; results from three experiments are plotted as the mean±SEM . Panel E shows the K_D (mean±SEM) values determined from three independent experiments.

Figure 3 Immunofluorescence analysis of internalization of CdtB CRAC mutants in Jurkat cells. Jurkat cells were exposed to media alone (grey curves), CdtA and CdtC alone (panel A), and CdtA and CdtC in the presence of $CdtB^{WT}$ (panel B), $CdtB^{V104P}$ (panel C), $CdtB^{Y105P}$ (panel D), $CdtB^{Y107P}$ (panel E) or $CdtB^{R110P}$ (panel F) for 1 hr and then

analyzed by immunofluorescence and flow cytometry for the presence of CdtB following fixation, permeabilization and staining with anti-CdtB mAb conjugated to AlexaFluor 488. Fluorescence is plotted versus relative cell number. Numbers represent the mean channel fluorescence (MCF); note that the MCF for cells not exposed to any Cdt peptide was 5.7. At least 10,000 cells were analyzed per sample; results are representative of three experiments.

Figure 4 Immunofluorescence analysis of internalization of CdtB CRAC mutants in THP-1 derived macrophages. Macrophages were exposed to media alone (grey curves), CdtA and CdtC alone (panel A), and CdtA and CdtC in the presence of $CdtB^{WT}$ (panel B), $CdtB^{V104P}$ (panel C), $CdtB^{Y105P}$ (panel D), $CdtB^{Y107P}$ (panel E) or $CdtB^{R110P}$ (panel F) for 1 hr and then analyzed by immunofluorescence and flow cytometry for the presence of CdtB following fixation, permeabilization and staining with anti-CdtB mAb conjugated to AlexaFluor 488. Fluorescence is plotted versus relative cell number. Numbers represent the mean channel fluorescence (MCF); note that the MCF for cells not exposed to any Cdt peptide was 8.6. At least 10,000 cells were analyzed per sample; results are representative of three experiments.

Figure 5 Immunofluorescence analysis of surface associated CdtC in Jurkat cells. Jurkat cells were exposed to media alone (grey curves), CdtA and CdtC alone (panel A), and CdtA and CdtC in the presence of $CdtB^{WT}$ (panel B), $CdtB^{V104P}$ (panel C), $CdtB^{Y105P}$

(panel D), $CdtB^{Y107P}$ (panel E) or $CdtB^{R110P}$ (panel F) for 30 min and then analyzed by immunofluorescence and flow cytometry for the presence of CdtC following fixation and staining with anti-CdtC mAb conjugated to AlexaFluor 488. Fluorescence is plotted versus relative cell number. Numbers represent the mean channel fluorescence (MCF); note that the MCF for cells not exposed to any Cdt peptide was 5.5. At least 10,000 cells were analyzed per sample; results are representative of three experiments.

Figure 6 Cumulative results of immunofluorescence assessment of CdtB internalization and Cdt binding. Panel A shows the results obtained from three experiments for internalization of CdtB in Jurkat cells. Panel B shows the results obtained from three experiments for internalization of CdtB in THP-1 cells. Panel C shows the results obtained from three experiments for holotoxin binding to the cell surface determined by immunofluorescence staining for the presence of CdtC in the absence of permeabilization. Results in each panel are expressed as a percentage of the MCF observed in $CdtB^{WT}$ and represent the mean±SEM; *denotes statistical significance ($P<0.05$) when compared to wildtype protein

Figure 7 Assessment of CdtB CRAC mutants for their ability to induce G2 arrest in Jurkat cells. Jurkat cells were exposed to medium alone or 10 ng/ml each of CdtA and CdtC in the presence of 0.8-20.0 ng/ml $CdtB^{WT}$ (panels A-C), $CdtB^{V104P}$ (panels D-

F), $CdtB^{Y105P}$ (panels G-I), $CdtB^{V107P}$ (panels J-L) or $CdtB^{R110P}$ (panels M-O). Cells were analyzed for cell cycle distribution 18 hrs after exposure to toxin subunits using flow cytometric analysis of propidium iodide fluorescence(28). The numbers in each panel represent the percentages of cells in the G2/M phase of the cell cycle. Cells exposed to medium alone exhibit 9.2% G2 cells and cells treated with only 10 ng/ml each of CdtA and CdtC exhibited 9.0% G2 cells (data not shown). Results are representative of three experiments.

Figure 8 Effect of CdtB CRAC mutants on DNA fragmentation in Jurkat cells. Jurkat cells were treated with10 ng/nl each of CdtA and CdtC in the presence of 0-20 ng/ml $CdtB^{WT}$ (●), $CdtB^{V104P}$ (▼), $CdtB^{Y105P}$ (▲), $CdtB^{Y107P}$ (■) or $CdtB^{R110P}$ (♦) for 48 hr. The cells were then analyzed by flow cytometry for the presence of DNA fragmentation as described in *Methods and Materials*. Results are plotted as net percent apoptotic cells versus CdtB concentration and represent the mean±SEM of three experiments; * indicates $P<0.05$ when compared to wildtype protein.

Figure 9 Effect of CdtB CRAC mutants on macrophage release of IL-1β and TNFα release. THP-1-derived macrophages were treated with 10 ng/ml each of CdtA and CdtC in the presence of 20 ng/ml $CdtB^{WT}$, $CdtB^{V104P}$, $CdtB^{Y105P}$, $CdtB^{Y107P}$ or $CdtB^{R110P}$ for 5 hr and the supernatants analyzed by ELISA for IL-1β (solid bars) and TNFα (hatched bars). Results are the mean ± SEM for three experiments each performed

in triplicate; *indicate $P<0.05$ when compared to $CdtB^{WT}$. Cells exposed to medium alone released 24.6±1.3 pg/ml IL-1β and168.2±17.9 pg/ml TNFα.

Figure 10 Assessment of CdtB CRAC mutants for PIP3 phosphatase activity. Varying amounts (0.25-1.0 μM) of $CdtB^{WT}$ (solid bars), $CdtB^{V104P}$ (left-hatched bars), $CdtB^{Y105P}$ (cross-hatched bars), $CdtB^{Y107P}$ (open bars) or $CdtB^{R110P}$ (right-hatched bars) were assessed for their ability to hydrolyze PI(3,4,5)-P_3 as described in *Materials and Methods*. The amount of phosphate release was measured using a malachite green binding assay. Data are plotted as phosphate release (nmol/30 min) versus protein concentration; results represent the mean ± SEM for three experiments each performed in triplicate; phosphatase activity exhibited by CdtB CRAC mutants was not statistically different from $CdtB^{WT}$.

Table 1

CdtB CRAC mutant constructs

Plasmid	Primer	Sequence[a]
pGEMCdtB^{V104P}	P1	CCGTCCAAATATGCCCTATATTTATTATTCCCG
	P2	CGGGAATAATAAATATAGGGCATATTTGGACGG
pGEMCdtB^{Y105P}	P3	GGTACTCGCTCCCGTCCAAATATGGTCCCTATTTATTATTCCCG
	P4	CGGGAATAATAAATAGGGACCATATTTGGACGGGAGCGAGTACC
pGEMCdtB^{Y107P}	P5	GGTCTATATTCCCTATTCCCGTTTAGATGTTGG
	P6	CCAACATCTAAACGGGAATAGGGAATATAGACC
pGEM CdtB^{R110P}	P7	GGTCTATATTTATTATTCCCCTTTAGATGTTGG
	P8	CCAACATCTAAAGGGGAATAATAAATATAGACC

Fig 1

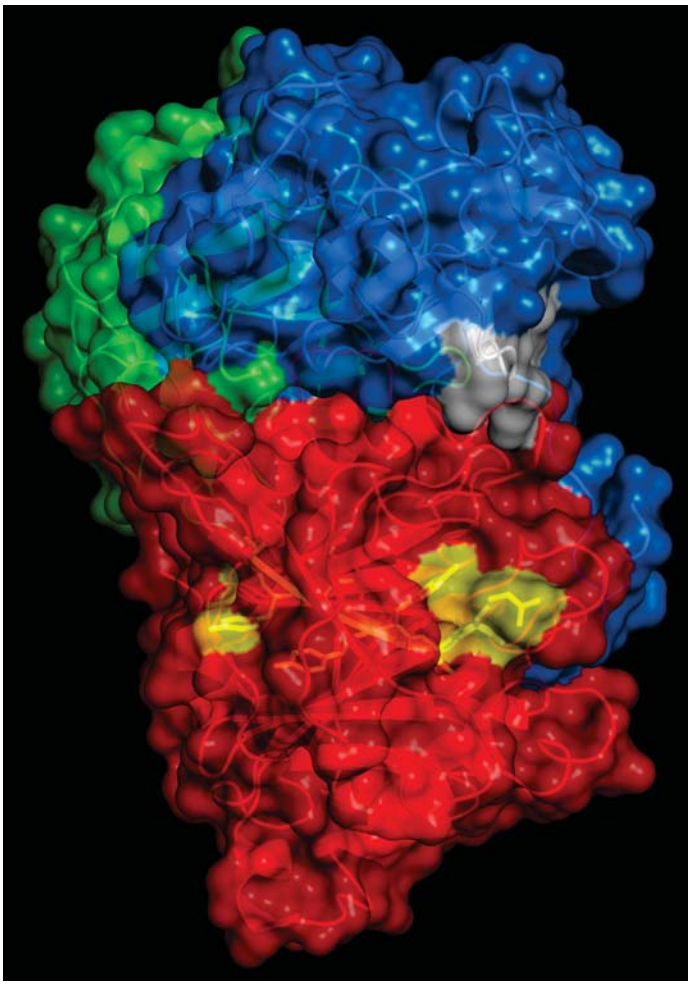

Fig 2

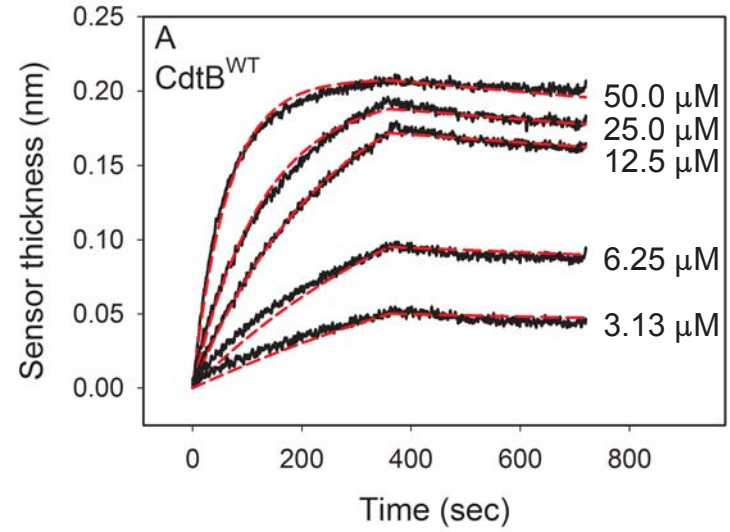

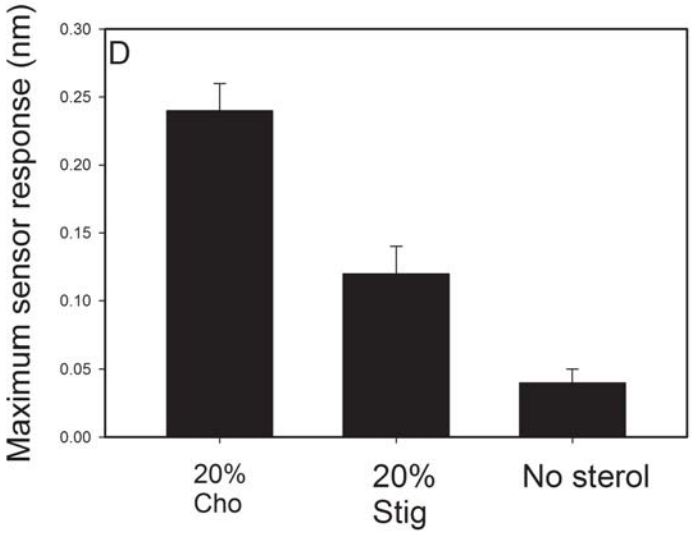

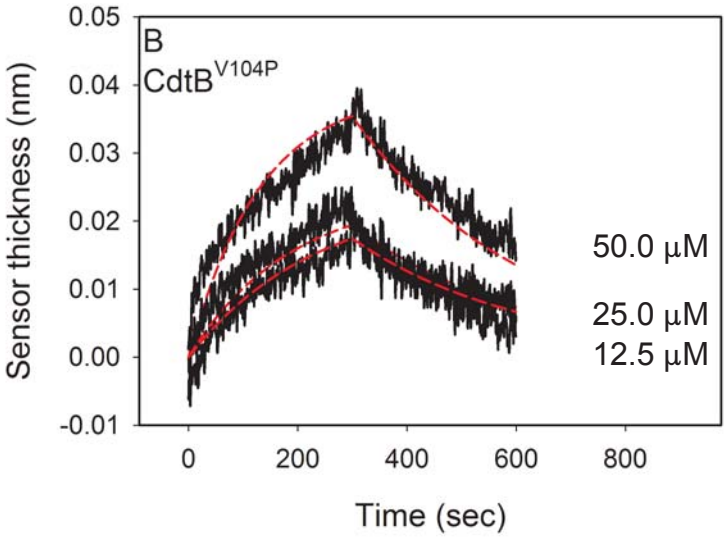

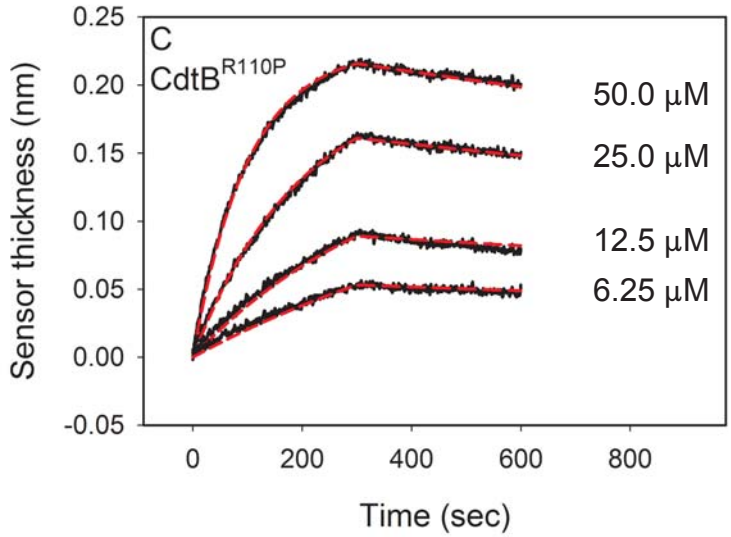

E
K_D values for CdtB CRAC mutants*

CdtB protein	K_D value
$CdtB^{WT}$	$1.37 \pm 0.2 \times 10^{-6}$
$CdtB^{V104P}$	$2.08 \pm 0.8 \times 10^{-5}$
$CdtB^{Y105P}$	ND
$CdtB^{Y107P}$	ND
$CdtB^{R110P}$	$3.35 \pm 1.9 \times 10^{-8}$

*K_D calculated based upon analysis of 3.1-50 µM protein; values represent mean ± S.E.M of three experiments and are statistically different (P <0.05) from $CdtB^{WT}$.
ND = K_D could not be determined

Fig 3

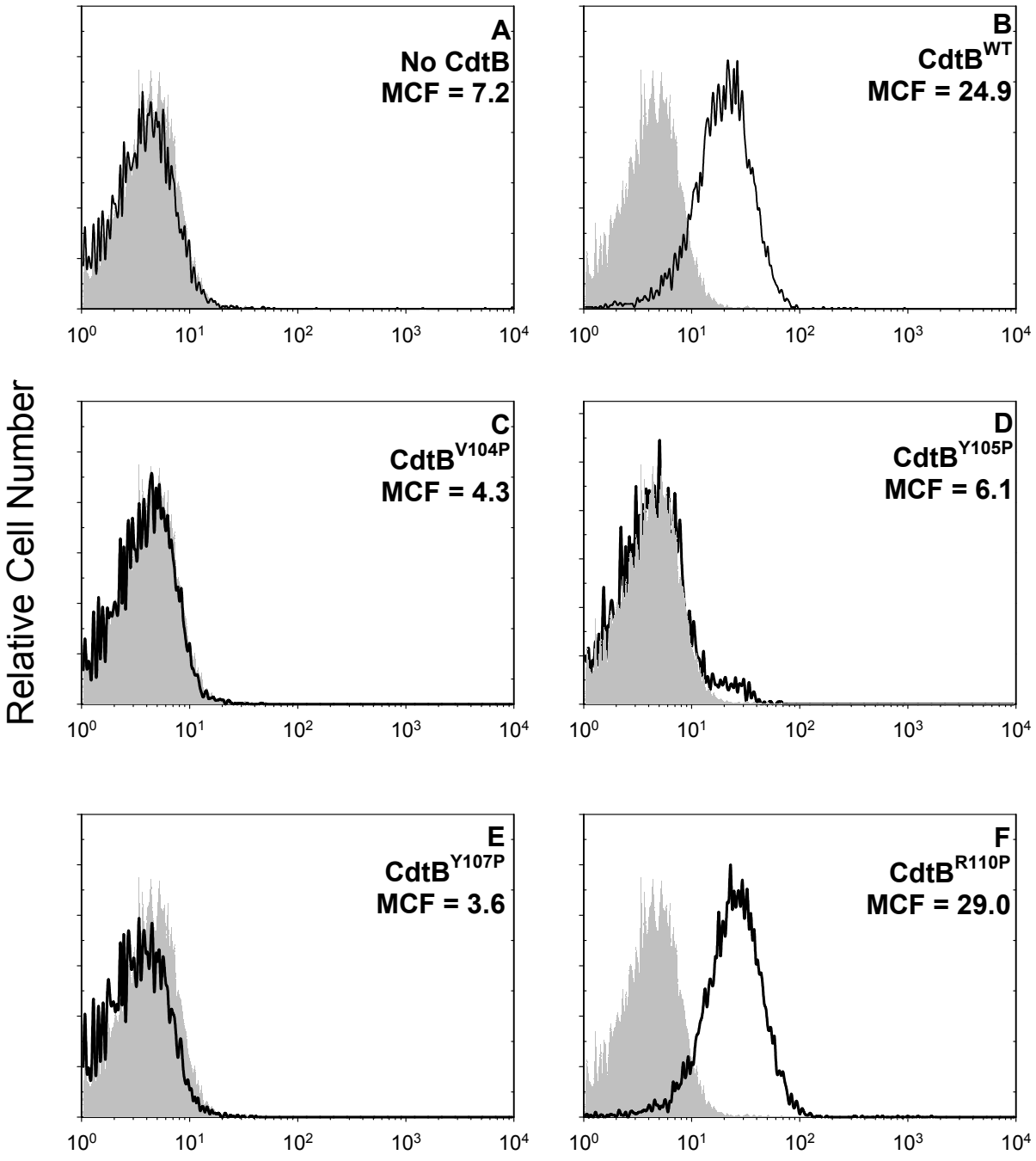
A
No CdtB
MCF = 7.2
B
CdtB^WT
MCF = 24.9
C
CdtB^V104P
MCF = 4.3
D
CdtB^Y105P
MCF = 6.1
E
CdtB^Y107P
MCF = 3.6
F
CdtB^R110P
MCF = 29.0
Relative Cell Number
Intracellular CdtB Fluorescence

Fig 4

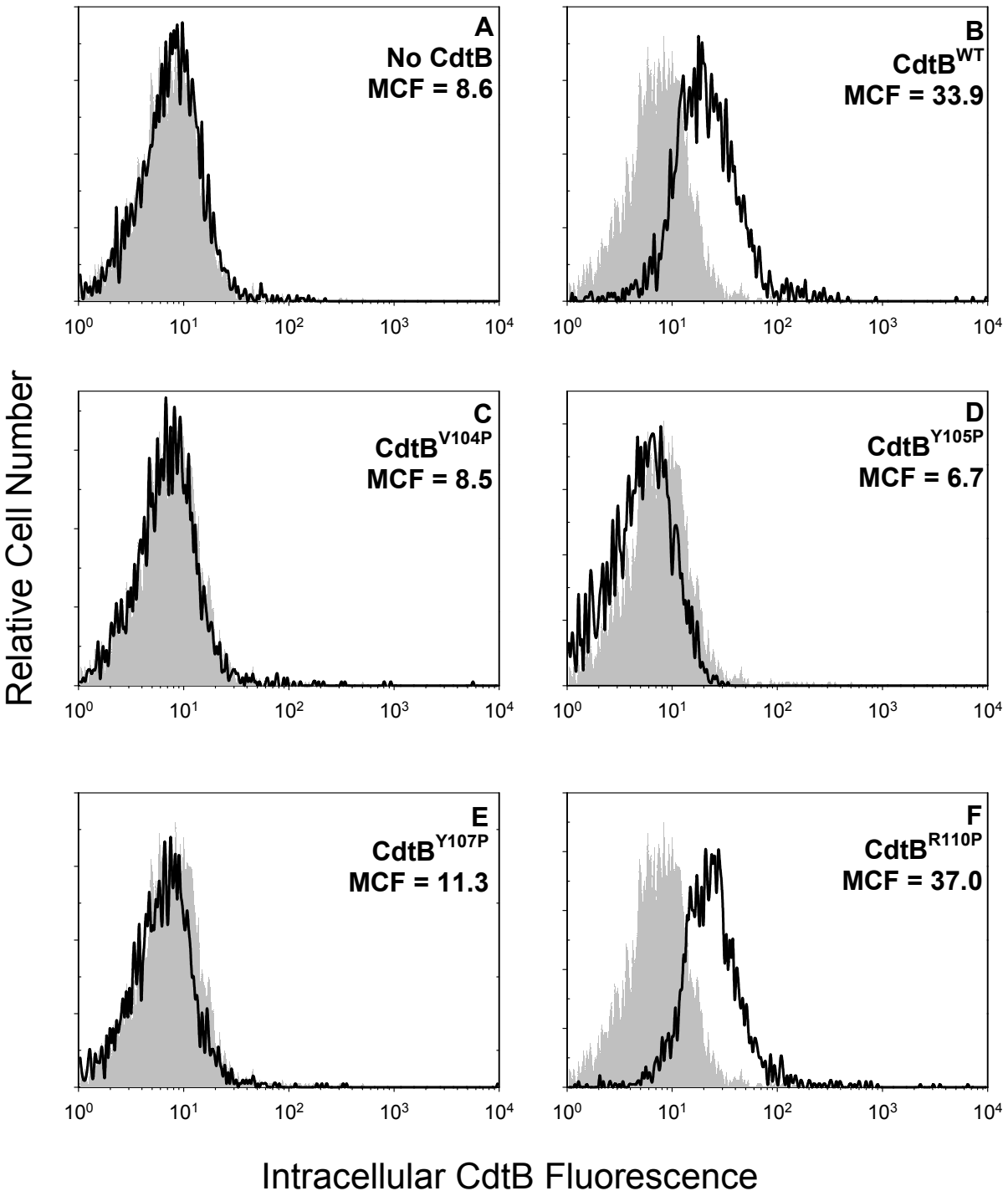
A
No CdtB
MCF = 8.6
B
CdtB^WT
MCF = 33.9
C
CdtB^V104P
MCF = 8.5
D
CdtB^Y105P
MCF = 6.7
E
CdtB^Y107P
MCF = 11.3
F
CdtB^R110P
MCF = 37.0
Relative Cell Number
Intracellular CdtB Fluorescence
10^0
10^1
10^2
10^3
10^4

Fig 5

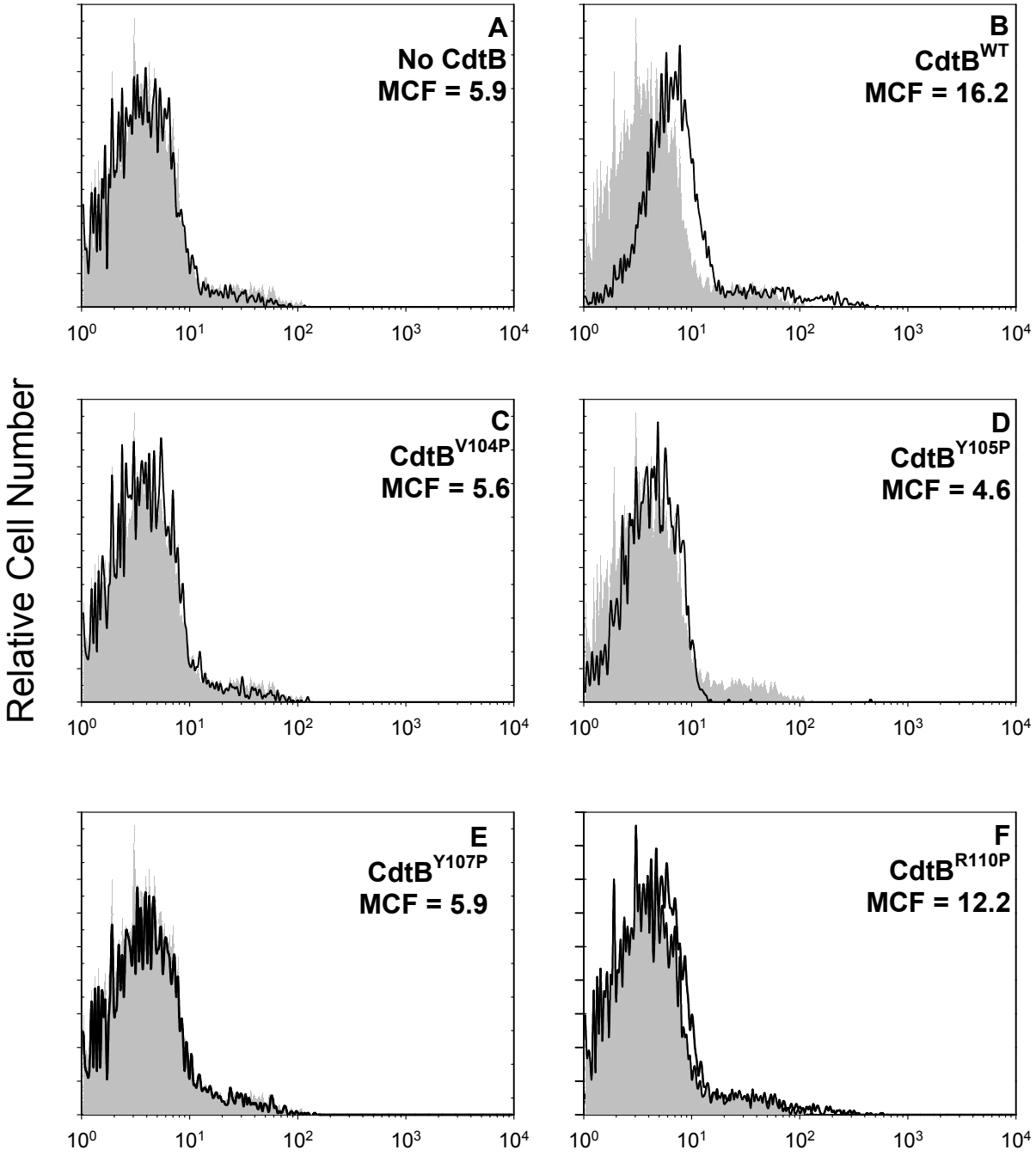
A
No CdtB
MCF = 5.9
B
CdtB^WT
MCF = 16.2
C
CdtB^V104P
MCF = 5.6
D
CdtB^Y105P
MCF = 4.6
E
CdtB^Y107P
MCF = 5.9
F
CdtB^R110P
MCF = 12.2
Relative Cell Number
Surface-associated CdtC Fluorescence

Fig 6

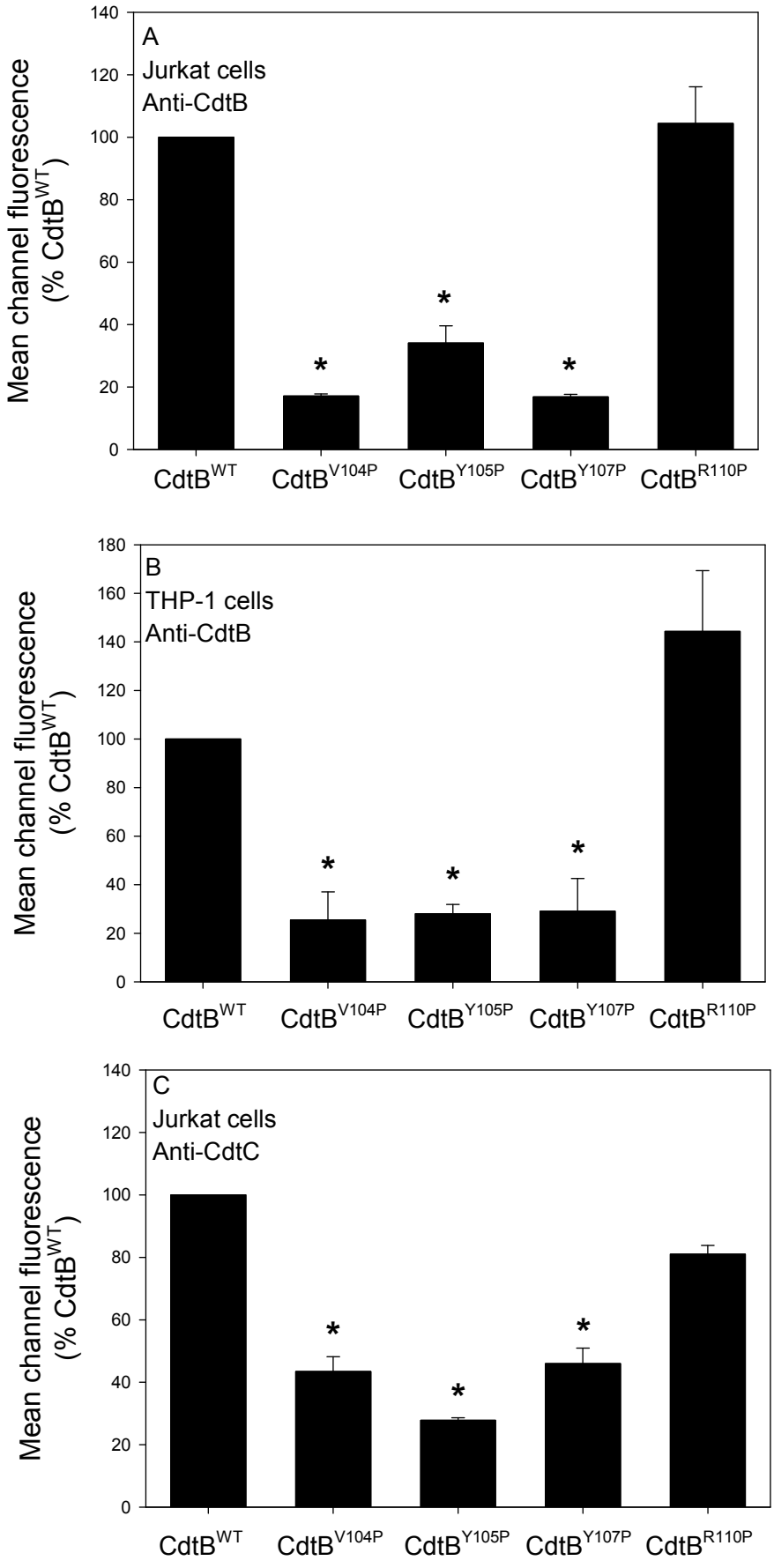
A
Jurkat cells
Anti-CdtB
Mean channel fluorescence (% CdtB^WT)
140
120
100
80
60
40
20
0
*
*
*
CdtB^WT
CdtB^V104P
CdtB^Y105P
CdtB^Y107P
CdtB^R110P
B
THP-1 cells
Anti-CdtB
Mean channel fluorescence (% CdtB^WT)
180
160
140
120
100
80
60
40
20
0
*
*
*
CdtB^WT
CdtB^V104P
CdtB^Y105P
CdtB^Y107P
CdtB^R110P
C
Jurkat cells
Anti-CdtC
Mean channel fluorescence (% CdtB^WT)
140
120
100
80
60
40
20
0
*
*
*
CdtB^WT
CdtB^V104P
CdtB^Y105P
CdtB^Y107P
CdtB^R110P

Fig 7

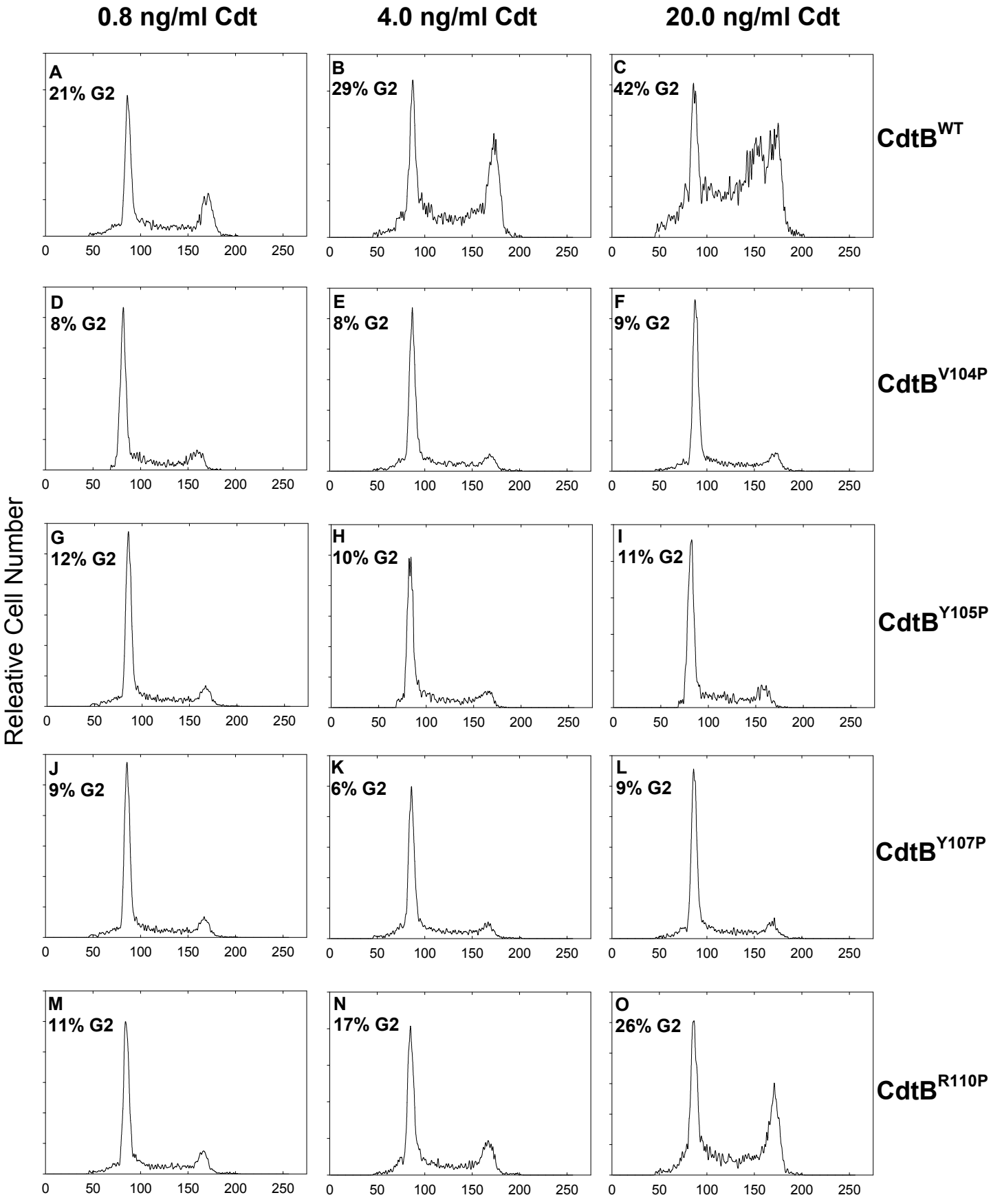
0.8 ng/ml Cdt
4.0 ng/ml Cdt
20.0 ng/ml Cdt
A
21% G2
B
29% G2
C
42% G2
CdtB^WT
D
8% G2
E
8% G2
F
9% G2
CdtB^V104P
G
12% G2
H
10% G2
I
11% G2
CdtB^Y105P
J
9% G2
K
6% G2
L
9% G2
CdtB^Y107P
M
11% G2
N
17% G2
O
26% G2
CdtB^R110P
Releative Cell Number
0 50 100 150 200 250
DNA Content
(Propidium iodide fluorescence)

Fig 8

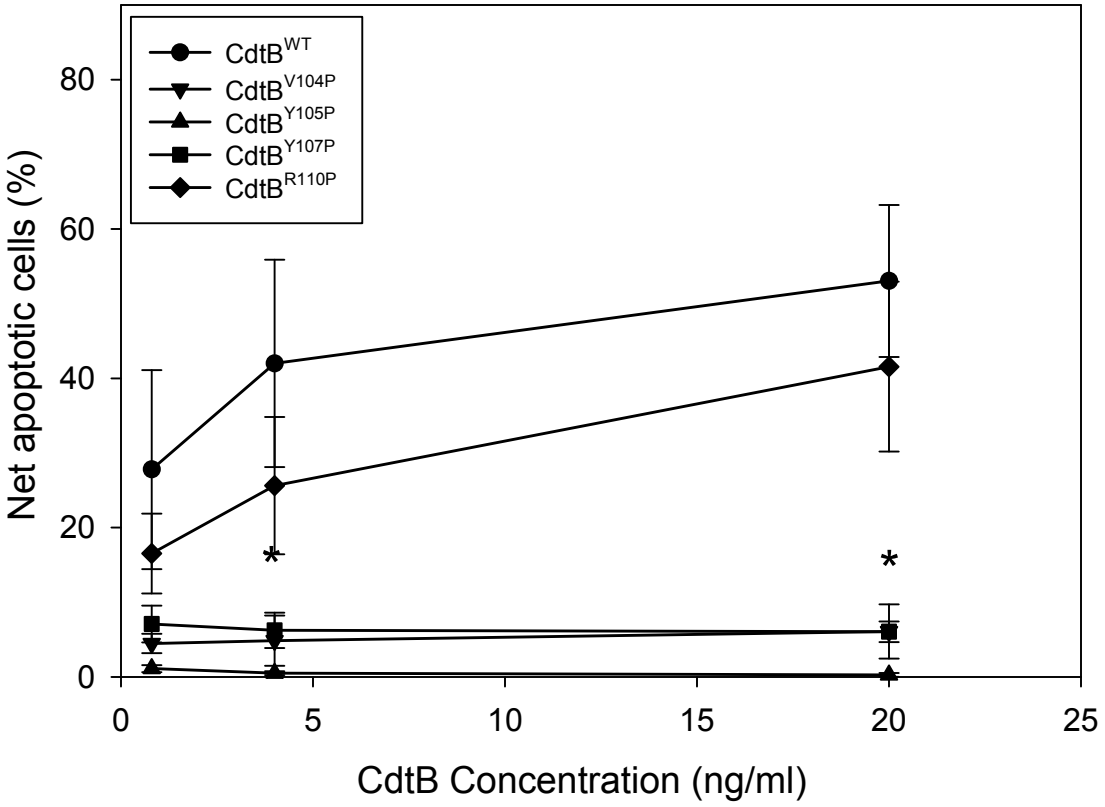
CdtB^WT
CdtB^V104P
CdtB^Y105P
CdtB^Y107P
CdtB^R110P
Net apoptotic cells (%)
0
20
40
60
80
0
5
10
15
20
25
CdtB Concentration (ng/ml)
*
*

Fig 9

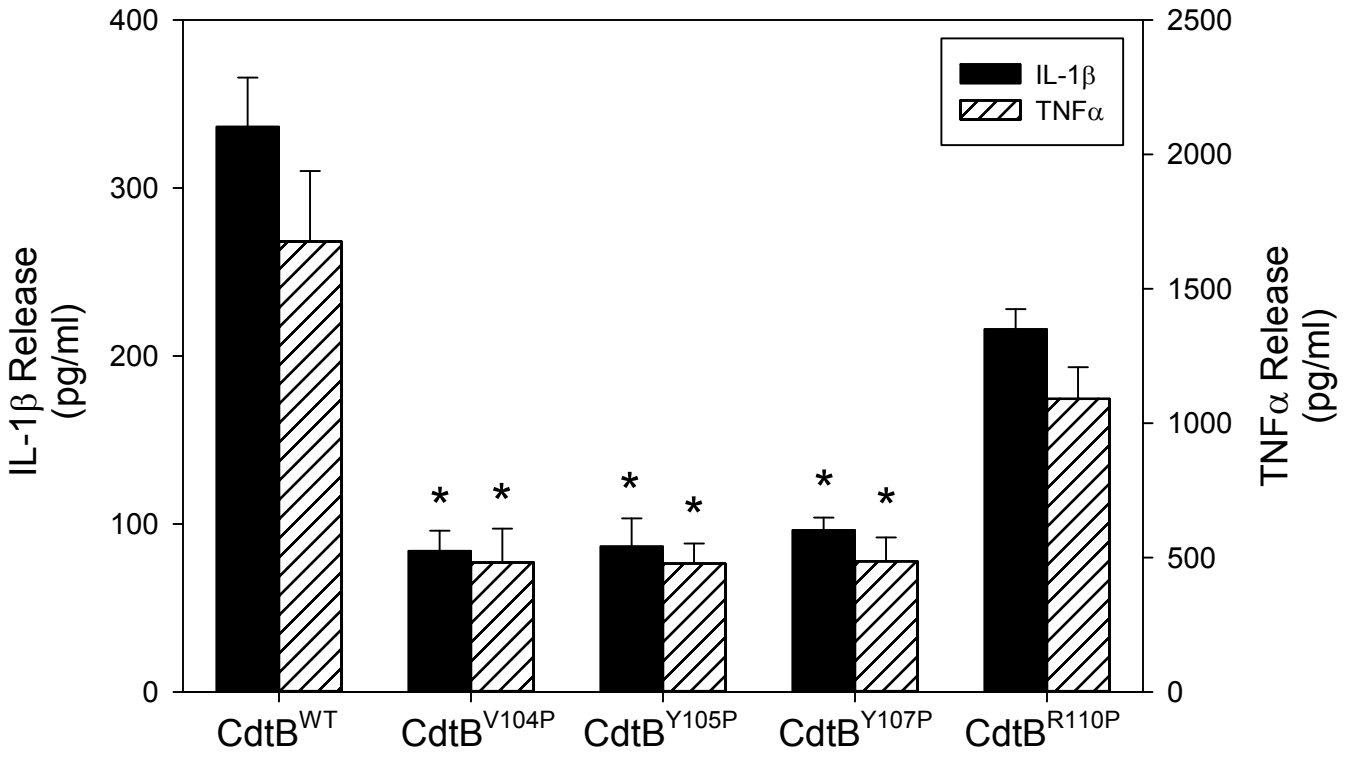
IL-1β Release (pg/ml)
TNFα Release (pg/ml)
IL-1β
TNFα
400
300
200
100
0
2500
2000
1500
1000
500
0
*
CdtB^WT
CdtB^V104P
CdtB^Y105P
CdtB^Y107P
CdtB^R110P

Fig 10

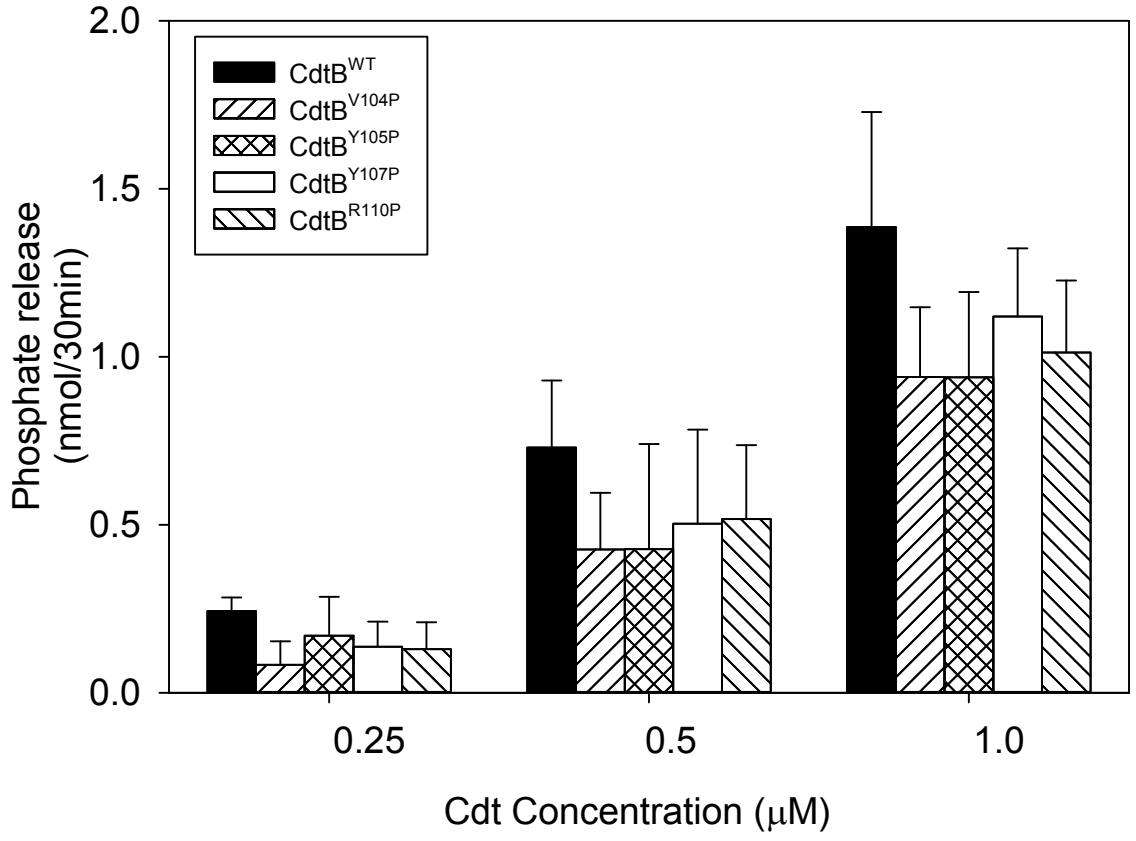
2.0
1.5
1.0
0.5
0.0
Phosphate release
(nmol/30min)
CdtB^WT
CdtB^V104P
CdtB^Y105P
CdtB^Y107P
CdtB^R110P
0.25
0.5
1.0
Cdt Concentration (μM)

Figure S1 BLI assessment of Cdt holotoxin binding to LUVs. LUVs containing PE-biotin were immobilized on streptavidin sensors and Cdt holotoxin served as the analyte. A representative BLI sensorgram is shown for the interaction of varying concentrations of Cdt holotoxin with LUVs containing 20% cholesterol; the experimental line (black) is shown along with the model fit (red line). The K_D value was determined to be 2.03×10^{-6} M.

Figure S2 CD analysis of $CdtB^{WT}$ and mutants. CD-data was collected on an Applied Photophysics Chirascan CD spectrometer at 25°C in a 1 mm quartz cuvette. Data was collected in 0.5 nm increments from 195-260 nm in 20 mM Sodium phosphate buffer, pH 7.4. The concentration was 100 µg/ml for $CdtB^{WT}$, $CdtB^{V104P}$, $CdtB^{Y105P}$, $CdtB^{R110P}$, and 50 µg/ml for $CdtB^{Y107P}$. All spectra are an average of three separate scans. None of the mutations had any effect on the secondary structure of CdtB

Figure S1

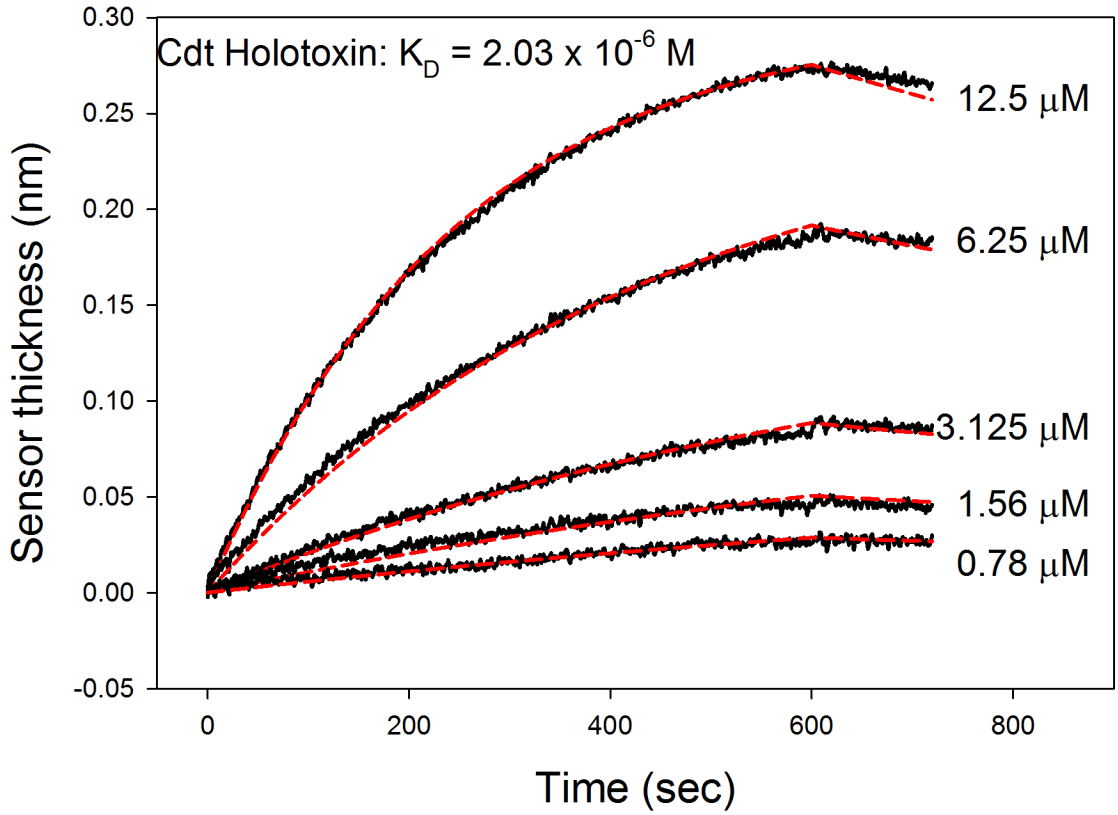
Cdt Holotoxin: K_D = 2.03 x 10^{-6} M
12.5 μM
6.25 μM
3.125 μM
1.56 μM
0.78 μM
Sensor thickness (nm)
0.30
0.25
0.20
0.15
0.10
0.05
0.00
-0.05
0
200
400
600
800
Time (sec)

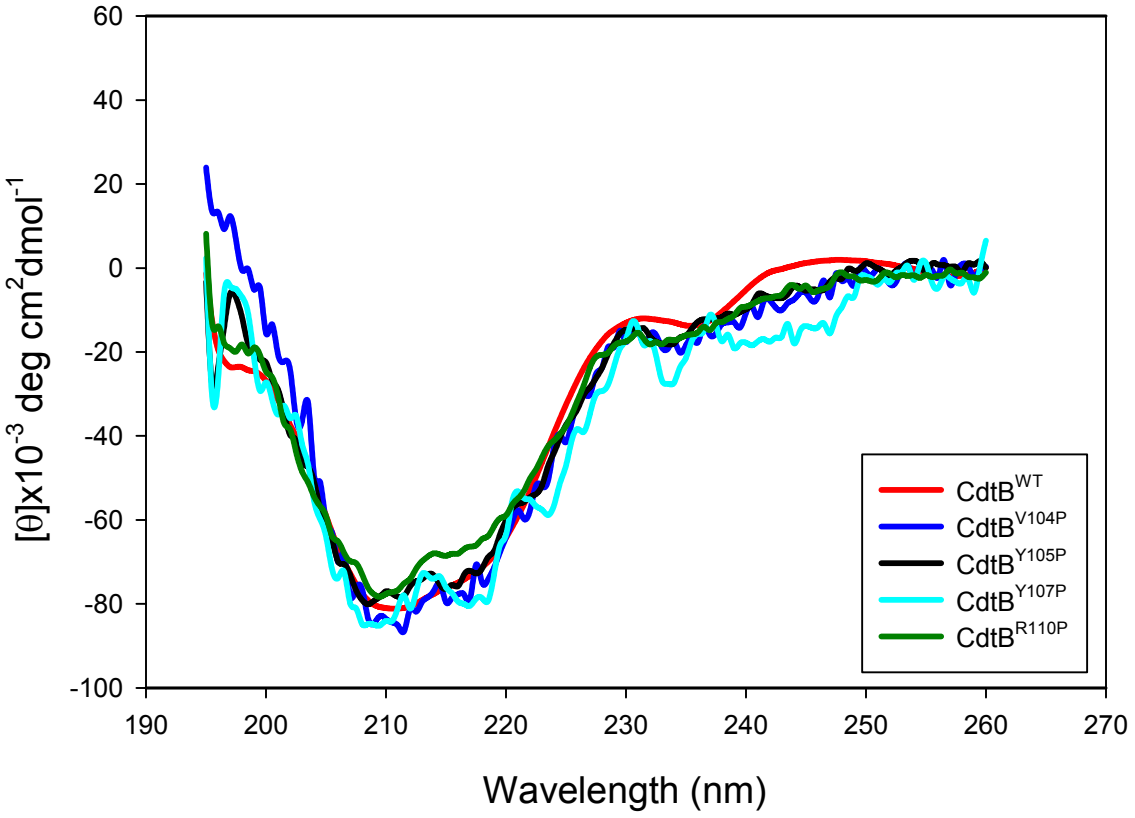
60
40
20
0
-20
-40
-60
-80
-100
190
200
210
220
230
240
250
260
270
[θ]x10-3 deg cm2dmol-1
Wavelength (nm)
CdtBWT
CdtBV104P
CdtBY105P
CdtBY107P
CdtBR110P